Analysis of scaling limits of the Kinetic Chemotaxis Equations

by

Ryan Thiessen

A thesis submitted in partial fulfillment of the requirements for the degree of

Masters of Science

in

Applied Mathematics

Department of Mathematical and Statistical Sciences
University of Alberta

Abstract

The kinetic chemotaxis equations have long been used to model biological processes. We will analyze a volume filling variant of the kinetic chemotaxis equations on the torus. Since the kinetic chemotaxis systems have well known blow-up solutions, we spend a considerable amount of time showing conditions for which solutions of the volume filling kinetic chemotaxis equations exist globally. Due to the individualist origins of the kinetic equation (velocity jump process), the system's interesting population dynamics occur at a much larger space-time scale. Various approximation methods have been developed to explore these population dynamics, like the parabolic scaling and moment closures. In this thesis, we will explore these approximation methods in the context of chemotaxis, and we will prove two new results for the convergence of the scaling limits to the parabolic limit and the hyperbolic limit, respectively. In addition to the approximation methods' mathematical consequences, we will delve into their underlying biological meaning, explain under what conditions the methods coincide, and discuss their differences. In developing these models, a few common features appear, such as anisotropic diffusion and chemotactic mixing. For the above macroscopic models, we develop a sophisticated numerical solver to investigate anisotropic pattern formation. To our surprise, we found new spatial criss-cross patterns due to competing cues, one direction given by anisotropy versus a different direction due to chemotaxis. A full analysis of these new patterns is not part of this thesis and is left for future work.

Acknowledgements

I would like to extend my deepest gratitude to my parents, for without them, I never would have gotten this far. I cannot begin to express my thanks to Thomas Hillen, for helping me with my research. I would also like to thank my sister for helping with editing. Finally, I want to thank NSERC for funding my research.

Table of Contents

1 Introduction **1**

2 Global Existence **6**

2.1 Local Existence and Uniqueness 8

2.2 P bounds 9

2.3 Classical Solutions for the Chemotaxis Equation 12

2.4 ∇S Energy estimates 16

2.5 Theorem 2: Global existence 22

3 Scaling Limits **25**

3.1 Parabolic Scaling 26

3.1.1 Rigorous Parabolic Limit 31

3.2 Hyperbolic Scaling 35

3.2.1 Rigorous Hyperbolic Limit 40

3.3 L^2 Moment Closure 43

3.4 Equilibrium Closure 47

3.5 Conclusion 51

3.5.1 Limit equations 51

4 Numerics **56**

4.1 Hybrid FVFD Scheme 56

4.2 Parameters 59

4.3 Vascular Network Formation 60

4.4 Anisotropic Diffusion 62

4.5 Chemotactic Mixing 64

4.6 Anisotropic Diffusion vs. Chemotactic mixing 65

5 Conclusion **67**

Bibliography **71**

List of Figures

4.1 Formation of Network: a) Initial condition with cell density of 100 $cells/mm^2$, b) Solution at $1.5s$ 61

4.2 Formation of Network: a) Initial condition with cell density of 200 $cells/mm^2$, b) Solution at $1.5s$ 61

4.3 Formation of Network: a) Initial condition with cell density of 400 $cells/mm^2$, b) Solution at $1.5s$ 62

4.4 Concentration parameter of $k = 5$: a) Initial condition with cell density of 200 $cells/mm^2$, b) Final State at $0.32s$ 63

4.5 Concentration parameter of $k = 10$: a) Initial condition with cell density of 200 $cells/mm^2$, b) Final State at $0.32s$ 63

4.6 Concentration parameter of $k = k(\mathbf{x})$: a) Initial condition with cell density of 200 $cells/mm^2$, b) Solution at $0.32s$ 64

4.7 Velocity mixing a) Initial condition with cell density of 200 $cells/mm^2$, b) Solution at $0.32s$ 64

4.8 Anisotropic Diffusion and Velocity Mixing: a) Initial condition with cell density of 200 $cells/mm^2$, b) Solution at 0.0989 s c) Solution at 0.32 s 65

Chapter 1

Introduction

This work aims to develop and analyze a set of equations describing cell movement in the presence of a chemoattractant. The motivating example is vascular assembly, where endothelial cells form a network of size invariant units called capillaries. The process of forming these networks is seen to be a cell-autonomous process that is permissive in the extracellular environment. In Preziosi's paper [47], it was shown that the endothelial cells' individual trajectories are highly directional towards zones of higher cell concentration. They found that this highly directional movement was produced by a chemoattractant (VEG-F), that the endothelial cells were producing. The cells also exhibit a particular type of motion known as 'run and tumble,' which has been studied extensively in *E. coli* [3, 4], 'run and tumble' motion can be described as a cell moving at a velocity for some time (run), then the cell stops and randomly chooses a new velocity (tumble). The resulting patterns created by *E. coli* have been exhaustively studied [2, 55, 7, 6]. From here, we can create a model by the assumption that cell movement can be modelled by a velocity jump process that is influenced by a chemoattractant [47]. The velocity jump process can be formalized by the following assumptions, the motion of each individual is piecewise linear, a run stops at a position with a given probability, and finally if an individual stops after a negligibly short time, it chooses a new direction with another given probability (for a more explicit derivation see [1]). We can arrive at a deterministic equation by integrating over suitable test domains and making use of Gauss' theorem [49]. After some computation,

we retrieve what is known as the transport equation in math biology literature [39] or the kinetic (Boltzmann type) equation in physics [10]

$$P_t(\mathbf{x}, \mathbf{v}, t) + \mathbf{v} \cdot \nabla_{\mathbf{x}} P(\mathbf{x}, \mathbf{v}, t) = \mathcal{L}P(\mathbf{x}, \mathbf{v}, t), \tag{1.1}$$

where $P = P(\mathbf{x}, \mathbf{v}, t)$ denotes the density of cells, and $\mathcal{L}$ is the turning operator, which represents the probability for a cell to change velocities. For simplicity, we are considering the spatial domain to be the torus, which we will denote as $x \in \mathbb{T}^n$, and the space of velocities that cells can take is a compact symmetric metric space $(V, |\cdot|^2)$. Compact for our purposes means that V is closed and bounded, and symmetric means that $\forall\ \mathbf{v} \in V \implies -\mathbf{v} \in V$. For calculations we will use the bounded sphere $V = [s_1, s_2] \times \mathbb{S}^{n-1}$, with $0 \leq s_1 \leq s_2 \leq \infty$.

The turning operator only involves cells changing velocity, and, therefore, should not affect the number of cells. Assuming that the number of cells remains the same, we gain the constraint on the turning operators

$$\int_V \mathcal{L}P(\mathbf{x}, \mathbf{v}, t) d\mathbf{v} = 0. \tag{1.2}$$

The corresponding conservation law can be obtained by integrating (1.1) over the velocity domain

$$\int_V P_t dv + \nabla_{\mathbf{x}} \cdot \int_V vP dv = \rho_t + \nabla_{\mathbf{x}} \cdot \mathbb{E}_p = 0, \tag{1.3}$$

where we define the density of cells at $(\mathbf{x}, t)$ as

$$\rho(\mathbf{x}, t) := \int_V P(\mathbf{x}, \mathbf{v}, t) d\mathbf{v},$$

and the first "moment" of P as

$$\mathbb{E}_p(\mathbf{x}, t) := \int_V \mathbf{v} P(\mathbf{x}, \mathbf{v}, t) d\mathbf{v}.$$

Remark 1 *For positive solutions of the kinetic equation [44] we have* $\|\rho_0\|_{L^1(\mathbb{T}^n)} = \|\rho\|_{L^1(\mathbb{T}^n)}$*, thanks to conservation of mass.*

Next for the form of the turning operator, a common form is

$$\mathcal{L}P = \mu \int_V T(\mathbf{x}, \mathbf{v}, \mathbf{v}')P(\mathbf{x}, \mathbf{v}', t)d\mathbf{v}' - \mu \int_V T(\mathbf{x}, \mathbf{v}', \mathbf{v})P(\mathbf{x}, \mathbf{v}, t)d\mathbf{v}',$$

the first term represents the flow of cell density from different velocities to $\mathbf{v}$, and the second term represents the flow from $\mathbf{v}$ to the other velocities. Fitting with our stochastic process from earlier, the kernel $T(\mathbf{x}, \mathbf{v}, \mathbf{v}')$ represents the probability of a cell switching to velocity $\mathbf{v}$ given it is currently moving at $\mathbf{v}'$. The constant μ is the rate at which the cells decide to switch velocity. We will assume that T does not depend on the incoming velocity. Cells tend to maintain a particular direction; however, for our model, we assume that the environment and chemical cues give the dominant directional cue. These assumptions allow us to simplify the expression

$$\mathcal{L}P = \mu T(\mathbf{x}, \mathbf{v})\rho(\mathbf{x}, t) - \mu P(\mathbf{x}, \mathbf{v}, t).$$

What is left to determine is the role in which a chemical signal will play on the model. For this, we make another assumption that the turning operator is a functional depending not only on the macroscopic cell density ρ, but also the concentration of the chemoattractant S and its gradient. We will denote this by $T := T[\rho, S](\mathbf{x}, \mathbf{v})$. Turning kernels of this type have been studied in [15, 20, 5, 32, 27]. The movement of the chemical signal is traditionally defined as a diffusion equation. However, depending on the time scale at which the chemoattractant diffuses, one can consider that chemoattractant is at equilibrium, then the resulting concentration is given by a Poisson type equation. Under this fast diffusion assumption, powerful results on existence and uniqueness have been obtained [15]. We take the traditional route and describe the motion as a diffusion equation, where the production of the chemoattractant is proportional to the cell density, and the chemoattractant degrades over time. These assumptions give us the diffusion equation

$$S_t = D_s \Delta S + \alpha\rho - \frac{1}{\tau}S. \tag{1.4}$$

Here, $S := S(\mathbf{x}, t)$ is the concentration of the chemoattractant, D_s is the

diffusion constant associated with how the chemoattractant moves through the environment, α is the rate of production of the chemoattractant by the cells, and τ is the rate of degradation of the chemoattractant.

Now recall the turning operator for our system

$$\mathcal{L}P(\mathbf{x},\mathbf{v},t) = -\mu P(\mathbf{x},\mathbf{v},t) + \mu \int_V T[S,\rho](\mathbf{x},\mathbf{v})P(\mathbf{x},\mathbf{v}',t)d\mathbf{v}', \tag{1.5}$$

this is still quite general; for our purposes, we can specify the operator further. These specifications take the form of splitting the environmental and chemoattractant effects, assuming that the cells sense the chemoattractant in a gradient along their velocity, and the cells are discouraged from aggregating to a single point. Putting these assumptions together, we arrive at the turning kernel

$$T[S,\rho] = q[\rho] + b[S](1-\rho)\mathbf{v}\cdot\nabla_{\mathbf{x}}S. \tag{1.6}$$

To fulfil the requirement that T is a probability distribution, we impose properties on b and q

$$\int_V q[\rho](\mathbf{v},\mathbf{x})d\mathbf{v} = 1, \quad \text{odd moments of } b[S](\mathbf{v},\mathbf{x}) \text{ equal zero}, \tag{1.7}$$

where q describes the environmental effects on the change of velocity. For example,environmental effects can include the extracellular matrix, other cells (volume filling), and fibres in which movement is easier for the cell to move along [29]. Hence, q depends explicitly on the location $\mathbf{x}$, and the velocity $\mathbf{v}$, with a functional dependence on the cell density ρ.

Remark 2 *Although it is a necessary condition for our model to make sense, we do not assume $T \geq 0$, $\forall \boldsymbol{x}, \boldsymbol{v}, t \in \mathbb{T}^n \times V \times \mathbb{R}_+$. The reasoning behind this is that we cannot a priori assign a sign to $\boldsymbol{v}\cdot\nabla S$. Under some assumptions on q and b we can show this positivity property, which an important subject of chapter 2.*

A good example of q is a fibre where movement is promoted along both directions

$$q(\mathbf{x},\mathbf{v}) = C(\mathbf{x})\left(e^{k\mathbf{v}\cdot\mathbf{u}} + e^{-k\mathbf{v}\cdot\mathbf{u}}\right) \tag{1.8}$$

where k is the concentration parameter, $\mathbf{u}$ is the the direction of the fibre, and $C(\mathbf{x})$ is the normalization constant. It is worth noting that the normalization constant is heavily dependent on the dimension [30]. The coefficient b in (1.6) describes the strength of the chemoattractant on the cell's velocity. Thus b depends explicitly on the location $\mathbf{x}$, and the velocity $\mathbf{v}$, with a functional dependence on the cell density S.

The example we will be looking at is

$$b(\mathbf{x}, \mathbf{v}) = \beta(\mathbf{x}) + \mathbf{v}^T A(\mathbf{x})\mathbf{v} \tag{1.9}$$

where β is the general sensing strength and $A(x)$ is a matrix that describes the directional dependence on sensing the chemoattractant. Back to the general theory, we can take advantage of the structure we have provided for ourselves, (1.5) simplifies to

$$\mathcal{L}P(\mathbf{x}, \mathbf{v}, t) = \mu(q[\rho](\mathbf{x}, \mathbf{v})\rho(\mathbf{x}, t) - P(\mathbf{x}, \mathbf{v}, t)) + \mu b[S](\mathbf{x}, \mathbf{v})(1 - \rho(\mathbf{x}, t))\mathbf{v} \cdot \nabla_{\mathbf{x}} S(\mathbf{x}, t). \tag{1.10}$$

Inputting this turning operator into (1.1), gives

$$\begin{aligned} P_t(\mathbf{x}, \mathbf{v}, t) + \mathbf{v} \cdot \nabla_{\mathbf{x}} P(\mathbf{x}, \mathbf{v}, t) &= \mu(q[\rho](\mathbf{x}, \mathbf{v})\rho(\mathbf{x}, t) - P(\mathbf{x}, \mathbf{v}, t)) \\ &\quad + \mu b[S](\mathbf{x}, \mathbf{v})\rho(\mathbf{x}, t)(1 - \rho(\mathbf{x}, t))\mathbf{v} \cdot \nabla_{\mathbf{x}} S(\mathbf{x}, t). \end{aligned} \tag{1.11}$$

We now have a mesoscopic set of equations; in the coming chapters, the goals are to show that solutions exist for this system, and for how long. Next, we examine various approximations and scaling limits and how they compare to each other. Finally, we explore numerics to get insight into pattern formation.

Chapter 2

Global Existence

We are now pulling together the previous equations (1.11), (1.4) and assumptions into a coherent formal system

$$P_t + (\mathbf{v}\cdot\nabla)P = \mu(q + b(1-\rho)\mathbf{v}\cdot\nabla S)\rho - \mu P, \in \mathbb{T}^n \times V \times \mathbb{R}_+ \tag{2.1}$$

$$S_t - D_s\Delta S = \alpha\rho - \frac{1}{\tau}S, \in \mathbb{T}^n \times \mathbb{R}_+ \tag{2.2}$$

$$P(\mathbf{x},\mathbf{v},0) = P_0(\mathbf{x},\mathbf{v}), \quad S(\mathbf{x},0) = 0. \tag{2.3}$$

For kinetic chemotaxis systems of this type, it is fairly easy to establish local in time existence and uniqueness (see the techniques in [43, 9]), but global existence for any chemotaxis system is always challenging. For this reason we consider a simplified model for this section where we drop the functional dependence of ρ and S on $q := q(\mathbf{v})$, and $b := b(\mathbf{x},\mathbf{v})$ while we establish global existence. Part of the reason why global existence for chemotaxis models is challenging is that blow-up solutions are common. For example, the famous chemotaxis model, the Keller Segel equations [35]

$$\begin{aligned} \rho_t &= \nabla(\nabla\rho - \rho\nabla S), \\ S_t &= \Delta S + \rho - S, \end{aligned} \tag{2.4}$$

has well-known blow-up solutions in dimensions greater than one [33]. The existence of blow-up solutions for reasonable parameter regimes has led to an

outpouring of modifications to this model that intend to model chemotaxis without infinite aggregations. A useful way to classify these new models is to combine the equation's classical PDE types (parabolic, hyperbolic, and elliptic) [19] of the model into a name, for example, the Keller-Segel equations (2.4) above is parabolic-parabolic type. In addition to the classical PDE classifications, we add kinetic for the kinetic equation, due to the different structure from the velocity dependence. The main equations (2.1) - (2.3) of this work are kinetic-parabolic.

For the kinetic - parabolic models, the goal is controlling the $\mathbf{v} \cdot \nabla S$ term in the turning kernel $T[\rho, S]$. The $\mathbf{v} \cdot \nabla S$ term is the main cause of the blow-up that occurs in chemotaxis systems. Heuristically, since S grows with the cell density, a gradient in the cell density induces a gradient in the chemoattractant, causing cells to move in that direction, making the gradient steeper. There are a couple of common methods to control this term; a method to use is non-local sensing of the chemoattractant to replace the local gradient [28]

$$\nabla S \to \mathring{\nabla} S := \frac{n}{|\mathbb{S}^{n-1}|R} \int_{\mathbb{S}^{n-1}} S(x + \nu R) d\nu. \tag{2.5}$$

Another method is where the chemoattractant is sensed at points in front and behind the cell

$$\nabla S \to \nabla S(\mathbf{x} + \epsilon \mathbf{v}, t) + \nabla S(\mathbf{x} - \epsilon \mathbf{v}, t), \tag{2.6}$$

These methods are quite successful at preventing blow-up [32, 5]. Last, there are the methods where the strength of the sensing is controlled, for instance, by encapsulating the gradient inside an arctan, thus bounding the chemotaxis term [46]; another method is to make the sensing density dependent[11]. In density-dependent sensing, the $\mathbf{v} \cdot \nabla S$ term is controlled by reducing the size or cutting off the term in regions of high density. We went with the density-dependent sensing, taking a volume filling form of $\rho(1 - \rho)$, which represents the physical reality that cells are not infinitely compressible [27]. In addition to this choice, we explore two cases where the time scale of the chemotaxis

degradation is on the same scale as the dynamics of the chemotactic signal

$$S_t = D_S \Delta S + \alpha\rho - \frac{1}{\tau} S, \tag{2.7}$$

and the case where it is much longer $\tau = \infty$

$$S_t = D_S \Delta S + \alpha\rho. \tag{2.8}$$

It is reasonable that in the $\tau < \infty$ case, global existence holds since the $\frac{1}{\tau}S$ helps reduce the size of ∇S. Whereas, in the $\tau = \infty$ case, this effect is absent. Instead, we rely on the dispersion of the Laplacian to reduce the ∇S, and therefore reduce aggregations of P.

For the goal of establishing global existence, we will follow [11] closely. The precise mathematical difficulty with dealing with the kinetic equation is the lack of *a priori* estimates; instead, we have to make use of the properties: 1) positivity, 2) mass conservation. Also, our only two properties are dependent on the positivity of the turning kernel [44]. Thus, our global solution is built on three steps. The first step is developing bounds for the kinetic equation based on a positivity assumption on some closed set $[0, t_*]$. The next step is based on using these local bounds to construct classical solutions for the parabolic chemotaxis equation, then constructing bounds on the challenging ∇S. Finally, since we have bounded solutions on $[0, t_*]$, the goal is to show $t_* = \infty$, thereby gaining a condition for which global solutions exist, completing the proof.

2.1 Local Existence and Uniqueness

We assume that (P_0, S_0) are chosen such that $0 < T[\rho, S](\mathbf{x}, \mathbf{v}) \leq 1, \quad \forall \mathbf{x}, \mathbf{v}, \in \mathbb{T}^n \times V$. Denoting this set of initial conditions as

$$\mathcal{G} := \{(P, S) \in L^2(\mathbb{T}^n \times V) \times L^2(\mathbb{T}^n) : 0 < T[\bar{P}, S](\mathbf{x}, \mathbf{v}) \leq 1, \quad \forall \mathbf{x}, \mathbf{v} \in \mathbb{T}^n \times V\}, \tag{2.9}$$

in addition we define the following Hilbert space

$$\mathcal{F} := \{(P,S) \in L^2(\mathbb{T}^n \times V) \times L^2(\mathbb{T}^n) : P(\cdot, v) \in H^1(\mathbb{T}^n),\ S \in H^2(\mathbb{T}^n)\}. \quad (2.10)$$

Defining $\mathcal{X} := \mathcal{F} \cap \mathcal{G}$ as our phase space, which is a closed subspace of $H^1(\mathbb{T}^n) \times H^2(\mathbb{T}^n)$.

Theorem 1 *(Local Existence and Uniqueness) if $(P_0, S_0) \in \mathcal{X}$, and T is continuous from this phase space $\mathcal{X}$ to $\mathbb{R}$ for each $(\boldsymbol{x}, \boldsymbol{v}) \in \mathbb{T}^n \times V$, then has a unique mild solution $(P,S) \in C([0,T] : \mathcal{F})$*

Proof:
Let $y := (P,S)$ then (2.1) - (2.3) can be written as

$$y_t + Ay + By = g(y), \quad (2.11)$$

where

$$A := \begin{pmatrix} (v \cdot \nabla) & 0 \\ 0 & \Delta \end{pmatrix}, \quad B := \begin{pmatrix} \mu & 0 \\ 0 & \tau^{-1} \end{pmatrix}, \quad g(y) := \begin{pmatrix} \mu T[\rho, S]\rho \\ \alpha\rho \end{pmatrix}. \quad (2.12)$$

We can show that $A+B$ generates a C^0 semigroup on $\mathcal{X}$. We begin by breaking down A into its components, where $\mathbf{v}\cdot\nabla$ is the shift operator which $i\mathbf{v}\cdot\nabla$ is self adjoint, and therefore generates a C_0 semigroup on $H^1(\mathbb{T}^n)$ via Stone's theorem. Now Δ generates the well known heat C_0 semigroup on $H^2(\mathbb{T}^n)$ [42], and we can analyze the components since the operators are linearly independent.

Now B is linearly bounded therefore $A + B$ generates a semigroup[42]. Since $T \leq 1$, $g(y)$ is locally Lipschitz then by Thm (6.1.4)[42] (2.11) has a unique mild solution and $y \in C([0,T] : \mathcal{F})$. as required. $\square$

2.2 P bounds

Now that we have local existence and uniqueness the goal is to acquire bounds on the kinetic equation, using a translational symmetry.

Lemma 1 *If (S,P) are solutions to* (2.1) - (2.3) *as in Theorem 1,* $P_0(\boldsymbol{x}, \boldsymbol{v}) = q(\boldsymbol{v})\rho_0(\boldsymbol{x})$*, and* $T[\rho, S](\boldsymbol{x}, \boldsymbol{v}) \geq 0, \quad \forall(\boldsymbol{x}, \boldsymbol{v}, t) \in \mathbb{T}^n \times V \times [0, t_*]$*, then*

$$P(\boldsymbol{x}, \boldsymbol{v}, t) \leq q(\boldsymbol{v}), \quad \rho(\boldsymbol{x}, t) \leq 1, \quad \forall(\boldsymbol{x}, \boldsymbol{v}, t) \in \mathbb{T}^n \times V \times [0, t_*]. \tag{2.13}$$

Proof:

Case 1: $\tau = \mathcal{O}(1)$

Consider the transformation

$$\tilde{P} = q - P, \quad \tilde{\rho} = \int_V \tilde{P} d\mathbf{v} = 1 - \rho, \tag{2.14}$$

$$\tilde{S} = \alpha\tau - S. \tag{2.15}$$

Substituting this change of variables into the kinetic-chemotaxis system (2.1) - (2.3)

$$(q - \tilde{P})_t + \mathbf{v} \cdot \nabla(q - \tilde{P}) = \mu \left((q - b\tilde{\rho}\mathbf{v} \cdot \nabla\tilde{S})(1 - \tilde{\rho}) - (q - \tilde{P}) \right), \tag{2.16}$$

$$-\tilde{P}_t - \mathbf{v} \cdot \nabla\tilde{P} = -\mu \left((q\tilde{\rho} + b(1 - \tilde{\rho})\tilde{\rho}\mathbf{v} \cdot \nabla\tilde{S}) - \tilde{P}) \right), \tag{2.17}$$

$$\tilde{P}_t + \mathbf{v} \cdot \nabla\tilde{P} = \mu \left((q\tilde{\rho} - b(1 - \tilde{\rho})\tilde{\rho}\mathbf{v} \cdot \nabla\tilde{S}) - \tilde{P}) \right), \tag{2.18}$$

which is the same as kinetic equation. Onto the chemoattractant equation

$$(\alpha\tau - \tilde{S})_t = D_s\Delta(\alpha\tau - \tilde{S}) + \alpha(1 - \tilde{\rho}) - \frac{1}{\tau}(\alpha\tau - \tilde{S}), \tag{2.19}$$

simplifying

$$\tilde{S}_t = D_s\Delta\tilde{S} + \alpha\tilde{\rho} - \frac{1}{\tau}\tilde{S}. \tag{2.20}$$

Since this transformation preserves the system the transformed variables $(\tilde{P}, \tilde{S})$ have the same property of positivity for $T[\rho, S] \geq 0$. Therefore the new variables $(\tilde{P}, \tilde{S})$ are also positive on $t \in [0, t_*]$, giving the bounds

$$(q - P) \geq 0, \quad \implies \rho \leq 1. \tag{2.21}$$

The proof for the $\tau = \infty$ case

$$\begin{aligned} P_t + (\mathbf{v} \cdot \nabla)P &= \mu(q + b\rho(1-\rho)\mathbf{v} \cdot \nabla S)\rho - \mu P, \\ S_t &= D_S \Delta S + \alpha\rho, \end{aligned} \tag{2.22}$$

we instead make the transformation

$$\tilde{P} = q - P, \quad \tilde{\rho} = \int_V \tilde{P} d\mathbf{v} = 1 - \rho, \tag{2.23}$$

$$\tilde{S} = \alpha t - S. \tag{2.24}$$

The kinetic equation remains the same as before. Substituting the transform into the chemotactic equation gives

$$(\alpha t - \tilde{S})_t = D_s \Delta(\alpha t - \tilde{S}) + \alpha(1 - \tilde{\rho}), \tag{2.25}$$

evaluating the derivatives leads to

$$\alpha - \tilde{S}_t = -D_S \Delta \tilde{S} + \alpha - \alpha\tilde{\rho}, \tag{2.26}$$

and we arrive at

$$\tilde{S}_t = D_S \Delta \tilde{S} + \alpha\tilde{\rho}. \tag{2.27}$$

Since this transformation preserves the system, the transformed variables $(\tilde{P}, \tilde{S})$ have the same property of positivity for $T[\rho, S] \geq 0$. Therefore, the new variables $(\tilde{P}, \tilde{S})$ are also positive on $t \in [0, t_*]$, giving the bounds

$$(q - P) \geq 0, \quad \implies \rho \leq 1. \tag{2.28}$$

□

2.3 Classical Solutions for the Chemotaxis Equation

The next step of constructing a classical solution of the parabolic chemotaxis equation (2.2) requires us to find the fundamental solution. Since we are on a space with no boundary, the Fourier transform is an attractive way to construct the fundamental solution. For this reason, we introduce the Fourier transform on the torus, for ϕ sufficiently smooth

$$\hat{\phi}(\omega) := \int_{\mathbb{T}^n} \phi(\mathbf{x}) e^{-i2\pi\omega\cdot\mathbf{x}} d\mathbf{x}, \quad \omega \in \mathbb{Z}^n, \tag{2.29}$$

with the inverse

$$\phi(\mathbf{x}) = \sum_{\omega\in\mathbb{Z}^n} \hat{\phi}(\omega) e^{i2\pi\omega\cdot\mathbf{x}}. \tag{2.30}$$

For details on Fourier transform properties, like the inversion theorem, and the convolution theorem, we point to the resource [51]. At first glance, it is unclear why (2.30) inverts the Fourier transform on the torus. We can gain intuition from considering a sufficiently smooth ϕ

$$\begin{aligned}
\phi(\mathbf{x}) &= \sum_{\omega\in\mathbb{Z}^n} \hat{\phi}(\omega) e^{i2\pi\omega\cdot\mathbf{x}}, \\
&= \sum_{\omega\in\mathbb{Z}^n} \int_{\mathbb{T}^n} \phi(\mathbf{y}) e^{-i2\pi\omega\cdot\mathbf{y}} d\mathbf{y} e^{i2\pi\omega\cdot\mathbf{x}}, \\
&= \sum_{\omega\in\mathbb{Z}^n} \int_{\mathbb{T}^n} \phi(\mathbf{y}) e^{i2\pi\omega\cdot(\mathbf{x}-\mathbf{y})} d\mathbf{y}.
\end{aligned}$$

moving the sum into the integral

$$\phi(\mathbf{x}) = \int_{\mathbb{T}^n} \phi(\mathbf{y}) \sum_{\omega\in\mathbb{Z}^n} e^{i2\pi\omega\cdot(\mathbf{x}-\mathbf{y})} d\mathbf{y}.$$

What is left to show is that the factor

$$\sum_{\omega\in\mathbb{Z}^n} e^{i2\pi\omega\cdot(\mathbf{x}-\mathbf{y})},$$

is a representation of the Dirac delta function on the torus. For this, we define the partial sum called the *Dirichlet Kernel* on $\mathbb{T}^1$ [38]

$$D_N(x) := \sum_{k=-N}^{N} e^{i2\pi kx}. \tag{2.31}$$

We can explicitly compute the sum by recalling the finite geometric series formula [38]

$$D_N(x) = \frac{\sin(2(N+1)\pi x)}{\sin(\pi x)}.$$

In the limit as $N \to \infty$, D_N happens to be one of the many representations of the delta function [38]

$$\lim_{N\to\infty} \frac{\sin(2(N+1)\pi x)}{\sin(\pi x)} = \delta(x). \tag{2.32}$$

It is clear that this result translates to higher dimensions, substituting this result into $\phi(\mathbf{x})$,

$$\int_{\mathbb{T}^n} \phi(\mathbf{y})\delta(\mathbf{x}-\mathbf{y})d\mathbf{y} = \phi(\mathbf{x}),$$

therefore, the inverse does invert the Fourier transform.

Using this definition, we can transform the chemoattractant equation and solve the resulting differential equation. Then use the Poisson summation formula to convert the resulting Fourier series into a series of Gaussians.

Lemma 2 *If $\rho \in L^\infty([0,t_*]; L^p(\mathbb{T}^n))$, $S_0 \in L^2(\mathbb{T}^n)$, $1 \le p \le \infty$, then*

$$S(x,t) = \int_{\mathbb{T}^n} S_0(y)G(x-y,t)dy + \alpha \int_0^t \int_{\mathbb{T}^n} \rho(y,s)G(x-y,t-s)dyds, \tag{2.33}$$

where for case $\tau = \mathcal{O}(1)$

$$G(x,t) := \left(\frac{\pi}{D_s t}\right)^{n/2} e^{-t/\tau} \sum_{\omega\in\mathbb{Z}^n} e^{-\pi^2 \frac{|x+w|^2}{D_s t}} \tag{2.34}$$

satisfies the equation in a classical sense for $t \leq t_*$

$$S_t - D_s \Delta S = \alpha\rho - \frac{1}{\tau} S \tag{2.35}$$

and for $\tau = \infty$

$$G(x,t) := \left(\frac{\pi}{D_s t}\right)^{n/2} \sum_{\omega \in \mathbb{Z}^n} e^{-\pi^2 \frac{|x+w|^2}{D_s t}} \tag{2.36}$$

satisfies the equation in a classical sense for $t \leq t_*$

$$S_t - D_s \Delta S = \alpha\rho \tag{2.37}$$

Proof:
Consider the spatial Fourier transform of the diffusion equation,

$$\hat{S}_t + \left(D_s |w|^2 + \frac{1}{\tau}\right) \hat{S} = \alpha \hat{\rho}. \tag{2.38}$$

Solving this ODE yields,

$$\hat{S} = \hat{S}_0 e^{-(D_s|w|^2 + 1/\tau)t} + \alpha \int_0^t e^{-(D_s|w|^2+1/\tau)(t-s)} \hat{\rho}(w,s) ds. \tag{2.39}$$

Transforming back gives

$$S = \sum_{\omega \in \mathbb{Z}^n} \hat{S}_0(\omega) e^{-(D_S|\omega|^2 + \frac{1}{\tau})t} e^{i2\pi\omega\cdot\mathbf{x}} + \alpha \sum_{\omega \in \mathbb{Z}^n} \int_0^t \hat{\rho}(\omega, s) e^{-(D_S|\omega|^2+\frac{1}{\tau})(t-s)} ds e^{i2\pi\omega\cdot\mathbf{x}}. \tag{2.40}$$

Now to determine the convergence of the Fourier series, we consider the first term

$$\begin{aligned} \left| \sum_{\omega \in \mathbb{Z}^n} \hat{S}_0(\omega) e^{-(D_S|\omega|^2 + \frac{1}{\tau})t} e^{i2\pi\omega\cdot\mathbf{x}} \right| &\leq \sum_{\omega \in \mathbb{Z}^n} |\hat{S}_0(\omega) e^{-(D_S|\omega|^2+\frac{1}{\tau})t}| \\ &\leq \left(\sum_{\omega \in \mathbb{Z}^n} |\hat{S}_0(\omega)|^2 \right)^{\frac{1}{2}} \end{aligned} \tag{2.41}$$

since $S_0 \in L^2(\mathbb{T}^n)$. This implies $\hat{S}_0 \in l^2(\mathbb{Z}^n)$. Therefore, the first term con-

verges. For the next term we have

$$\begin{aligned}&\left|\sum_{\omega\in\mathbb{Z}^n}\int_0^t \hat{\rho}(\omega,s)e^{-(D_S|\omega|^2+\frac{1}{\tau})(t-s)}dse^{i2\pi\omega\cdot\mathbf{x}}\right| \\ &\leq \sup_{s\in[0,t]}\|\hat{\rho}(\cdot,s)\|_{l^\infty(\mathbb{Z}^n)}\sum_{\omega\in\mathbb{Z}^n}\left(\frac{1-e^{-(D_s|\omega|^2+1/\tau)t}}{D_s|\omega|^2+1/\tau}\right).\end{aligned} \tag{2.42}$$

Since we have that $\rho\in L^1(\mathbb{T}^n)$ which through the Riemann–Lebesgue *Lemma* implies $\hat{\rho}\in l^\infty(\mathbb{Z}^n)$ [51], and since $\sum_{\omega\in\mathbb{Z}^n}\frac{1}{|\omega|^2+a}$ converges, this Fourier series also converges. Now consider the summation kernel

$$\hat{G}(\omega,t):=e^{-(D_s|\omega|^2+1/\tau)t}. \tag{2.43}$$

This function takes $\hat{G}:\mathbb{Z}^n\times\mathbb{R}_+\to\mathbb{R}$, but we can extend the inputs from $\mathbb{Z}^n$ to $\mathbb{R}^n$. In this sense we can use the Poisson sum formula [51], i.e. $f\in L^1(\mathbb{R}^n)\cap C(\mathbb{R}^n)$, then

$$F(\mathbf{x}):=\sum_{\omega\in\mathbb{Z}^n}f(\mathbf{x}+\omega)=\sum_{\omega\in\mathbb{Z}^n}\hat{f}(\omega)e^{2\pi i\omega\cdot\mathbf{x}}. \tag{2.44}$$

Note $F(\mathbf{x})$ is scalar function on the torus. To use the Poisson summation formula, we need to know the inverse Fourier transform of the Gaussian on $\mathbb{R}^n$

$$\mathcal{F}^{-1}\left[e^{-(D_s|\omega|^2t)}\right]=\left(\frac{\pi}{D_st}\right)^{n/2}e^{-\pi^2\frac{|x|^2}{D_st}}, \tag{2.45}$$

which is a well known result [56]. Substituting the above Fourier transform into the Poisson Summation formula we get

$$G(\mathbf{x},t):=\sum_{\omega\in\mathbb{Z}^n}e^{-(D_s|\omega|^2+1/\tau)t}e^{2\pi i\omega\cdot\mathbf{x}}=\left(\frac{\pi}{D_st}\right)^{n/2}e^{-t/\tau}\sum_{\omega\in\mathbb{Z}^n}e^{-\pi^2\frac{|x+w|^2}{D_st}}. \tag{2.46}$$

In addition, convergence of the Fourier series in $L^2(\mathbb{T}^n)$ gives free reign to use the convolution theorem

$$S=(S_0(\cdot)*G(\cdot,t))(\mathbf{x})+\alpha\int_0^t(\rho(\cdot,s)*G(\cdot,t-s))(x)ds. \tag{2.47}$$

In the $\tau = \infty$ case we arrive at nearly the same result, except for $e^{t/\tau} \to 1$. $\square$

2.4 ∇S Energy estimates

With a classical solution to the chemotaxis equation found, we can find estimates for ∇S.

Lemma 3 *If (S,P) are solutions to* (2.1) - (2.3) *as in Theorem 1,* $S_0 = 0$, $P_0 = \rho_0 q$, *and* $T[\rho, S](\boldsymbol{x}, \boldsymbol{v}) \geq 0, \quad \forall (\boldsymbol{x}, \boldsymbol{v}, t) \in \mathbb{T}^n \times V \times [0, t_*]$, *then for both* $\tau = \mathcal{O}(1)$ *and* $\tau = \infty$ *we have the estimate*

$$\|\nabla S\|_\infty \leq \alpha \frac{12}{2^{\frac{2}{3}}} \frac{c(n)}{D_s} \|\rho_0\|_{L^1(\mathbb{T}^n)} \tag{2.48}$$

where

$$c(n) := \frac{(\Gamma(\frac{n+1}{2}))^{\frac{2}{3}}}{\Gamma(\frac{n}{2})} \left(\frac{(n+4)^{\frac{n}{2}+2}}{2^{\frac{n}{2}}} \left(\frac{3+n}{3n} \right) e^{-\frac{n+4}{2}} \right)^{\frac{1}{3}} \tag{2.49}$$

Proof:
Consider the gradient fundamental solution of S

$$\nabla G(\mathbf{x}, t) = \sum_{\omega \in \mathbb{Z}^n} 2\pi\omega i e^{-(D_s|\omega|^2 + 1/\tau)t} e^{2\pi i \omega \cdot \mathbf{x}}. \tag{2.50}$$

Now let us examine the L^∞ norm of the above gradient

$$\begin{aligned} \|\nabla G(\mathbf{x}, t)\|_\infty &= \sup_{\mathbf{x} \in \mathbb{T}^n} \{ | \sum_{\omega \in \mathbb{Z}^n} 2\pi\omega i e^{-(D_s|\omega|^2 + 1/\tau)t} e^{2\pi i \omega \cdot \mathbf{x}} | \} \\ &\leq 2\pi e^{-t/\tau} \sum_{\omega \in \mathbb{Z}^n} |\omega| e^{-D_s|\omega|^2 t}. \end{aligned}$$

At this point, it is clear that $t = 0$ is an issue for $\|\nabla G(\cdot, t)\|_\infty$, since the sum $\sum_{\omega \in \mathbb{Z}^n} |\omega|$ will not converge. The estimate we are deriving is only valid for $t \in (0, t_*]$. For $t = 0$ we have that $S_0(\mathbf{x}) = 0, \ \forall x \in \mathbb{T}^n$, thus $\|\nabla S\|_\infty = 0$. Now

consider the Poisson Summation formula at $\mathbf{x} = 0$ (2.46)

$$G(0,t) = \sum_{\omega \in \mathbb{Z}^n} e^{-D_s|\omega|^2 t} = \left(\frac{\pi}{D_s t}\right)^{n/2} \sum_{\omega \in \mathbb{Z}^n} e^{-\pi^2 \frac{|\omega|^2}{D_s t}},$$

taking the radial derivative $\partial/\partial|\omega|$ of both sides

$$\frac{\partial}{\partial|\omega|} G(0,t) = \sum_{\omega \in \mathbb{Z}^n} -2D_s t|\omega| e^{-D_s|\omega|^2 t} = \left(\frac{\pi}{D_s t}\right)^{n/2} \sum_{\omega \in \mathbb{Z}^n} -\frac{2\pi^2}{D_s t}|\omega| e^{-\pi^2 \frac{|\omega|^2}{D_s t}},$$

thus we have

$$\sum_{\omega \in \mathbb{Z}^n} |\omega| e^{-D_s|\omega|^2 t} = \left(\frac{\pi}{D_s t}\right)^{\frac{n}{2}+2} \sum_{\omega \in \mathbb{Z}^n} |\omega| e^{-\pi^2 \frac{|\omega|^2}{D_s t}}. \tag{2.51}$$

Substituting this formula into the $\|\nabla G\|_\infty$ we have

$$\|\nabla G\|_\infty \leq 2\pi e^{-t/\tau} \left(\frac{\pi}{D_s t}\right)^{\frac{n}{2}+2} \sum_{\omega \in \mathbb{Z}^n} |\omega| e^{-\pi^2 \frac{|\omega|^2}{D_s t}}.$$

We can bound the sum by considering the radial symmetry of $|\omega| e^{-\pi^2 \frac{|\omega|^2}{D_s t}}$, and splitting the sum into increasing and decreasing parts

$$\sum_{\omega \in \mathbb{Z}^n} |\omega| e^{-\pi^2 \frac{|\omega|^2}{D_s t}} = 2^n \sum_{\omega \in \mathbb{Z}^n_+} |\omega| e^{-\pi^2 \frac{|\omega|^2}{D_s t}}. \tag{2.52}$$

At this point, we can view the above sum as Riemann sums of the integral

$$\int |\omega| e^{-\pi^2 \frac{|\omega|^2}{D_s t}} d\omega,$$

as either a right point or left point rule. For positive functions, we know that each monotonic piece of integrand can bound either the left or right point Riemann sum. The function $|\omega| e^{-\pi^2 \frac{|\omega|^2}{D_s t}}$ has very clear monotone regions, for $|\omega| \leq \left(\frac{D_s t}{2\pi^2}\right)^{\frac{1}{2}}$ it is increasing, and for $|\omega| > \left(\frac{D_s t}{2\pi^2}\right)^{\frac{1}{2}}$ it is decreasing. Then, we can make the following bounds, using the right point rule on $|\omega_j| \leq \left(\frac{D_s t}{2\pi^2}\right)^{\frac{1}{2}}$

region

$$\sum_{\omega\in\mathbb{Z}_+^n:|\omega_j|\leq\left(\frac{D_st}{2\pi^2}\right)^{\frac{1}{2}}} |\omega|e^{-\pi^2\frac{|\omega|^2}{D_st}} \leq \int_{\mathbb{R}_+^n:|\omega_j|\leq\left(\frac{D_st}{2\pi^2}\right)^{\frac{1}{2}}+1} |\omega|e^{-\pi^2\frac{|\omega|^2}{D_st}}d\omega, \tag{2.53}$$

and the left point rule on the $|\omega_j| > \left(\frac{D_st}{2\pi^2}\right)^{\frac{1}{2}}$ region

$$\sum_{\omega\in\mathbb{Z}_+^n:|\omega_j|>\left(\frac{D_st}{2\pi^2}\right)^{\frac{1}{2}}} |\omega|e^{-\pi^2\frac{|\omega|^2}{D_st}} \leq \int_{\mathbb{R}_+^n} |\omega|e^{-\pi^2\frac{|\omega|^2}{D_st}}d\omega. \tag{2.54}$$

In particular, we have

$$\sum_{\omega\in\mathbb{Z}_+^n} |\omega|e^{-\pi^2\frac{|\omega|^2}{D_st}} \leq 2\int_{\mathbb{R}_+^n} |\omega|e^{-\pi^2\frac{|\omega|^2}{D_st}}d\omega. \tag{2.55}$$

We convert now to spherical coordinates, which in n dimensions has the volume element

$$d\omega = |\omega|^{n-1}sin^{n-2}(\phi_1)sin^{n-3}(\phi_2)\cdots sin(\phi_{n-2})d|\omega|d\phi_1 d\phi_2\cdots d\phi_{n-1}. \tag{2.56}$$

Since our function has radial symmetry, we compute the angular terms [31]

$$\int_{\mathbb{S}^{n-1}} sin^{n-2}(\phi_1)sin^{n-3}(\phi_2)\cdots sin(\phi_{n-2})d\phi_1 d\phi_2\cdots d\phi_{n-1} = \frac{2\pi^{\frac{n}{2}}}{\Gamma(\frac{n}{2})} \tag{2.57}$$

Now, we compute the radial component

$$2\int_{\mathbb{R}^n} |\omega|e^{-\pi^2\frac{|\omega|^2}{D_st}}d\omega = \frac{4\pi^{\frac{n}{2}}}{\Gamma(\frac{n}{2})}\int_0^\infty |\omega|^n e^{-\pi^2\frac{|\omega|^2}{D_st}}d|\omega|, \tag{2.58}$$

changing variables $u = \frac{\pi^2|\omega|^2}{D_s t}$, we get

$$2\int_{\mathbb{R}^n} |\omega| e^{-\pi^2 \frac{|\omega|^2}{D_s t}} d\omega = \frac{4\pi^{\frac{n}{2}}}{\Gamma(\frac{n}{2})} \left(\frac{D_s t}{\pi^2}\right)^{\frac{n+1}{2}} \int_0^\infty u^{\frac{n+1}{2}-1} e^{-u} d|\omega|,$$
$$= 4\pi^{\frac{n}{2}} \frac{\Gamma(\frac{n+1}{2})}{\Gamma(\frac{n}{2})} \left(\frac{D_s t}{\pi^2}\right)^{\frac{n+1}{2}}.$$

Using this inequality to bound $\|\nabla G\|_\infty$ yields

$$\|\nabla G\|_\infty \leq 8\pi^{\frac{n}{2}+1} e^{-t/\tau} \left(\frac{\pi}{D_s t}\right)^{\frac{n}{2}+2} \left(\frac{D_s t}{\pi^2}\right)^{\frac{n+1}{2}} \frac{\Gamma(\frac{n+1}{2})}{\Gamma(\frac{n}{2})}, \tag{2.59}$$
$$\leq 8\pi^2 \left(\frac{1}{D_s t}\right)^{\frac{3}{2}} e^{-t/\tau} \frac{\Gamma(\frac{n+1}{2})}{\Gamma(\frac{n}{2})}. \tag{2.60}$$

Now, we can start moving towards the actual estimate using Holder's inequality, for a fixed $t_0 \in (0, t_*]$

$$\|\nabla S\|_\infty \leq \alpha \int_0^{t_0} \|\nabla G(\cdot, s)\|_\infty \|\rho(\cdot, t-s)\|_1 ds$$
$$+ \alpha \int_{t_0}^{t} \|\nabla G(\cdot, s)\|_\infty \|\rho(\cdot, t-s)\|_1 ds.$$

The first thing to note is that since P remains positive in the region $[0, t_*]$, we have $\|\rho\|_1 = \|\rho_0\|_1$ thanks to the conservation of mass property (**Remark 1**), allowing us to take $\|\rho(\cdot, t-s)\|_1$ out of the integral

$$\|\nabla S\|_\infty \leq \alpha \|\rho_0\|_1 \int_0^{t_0} \|\nabla G(\cdot, s)\|_\infty ds$$
$$+ \alpha \|\rho_0\|_1 \int_{t_0}^{t} \|\nabla G(\cdot, s)\|_\infty ds.$$

The next thing to note is that our bound for $\|\nabla G\|_\infty$ (2.59) is bounded in the integral from t_0 to t, but becomes unbounded near zero, therefore a different

bound is needed for the first integral. For this reason, consider the first integral

$$I = \int_0^{t_0} \|\nabla G(\cdot, s)\|_\infty ds = \int_0^{t_0} \sup_{\mathbf{x}\in\mathbb{T}^n} \{|\sum_{\omega\in\mathbb{Z}^n} 2\pi\omega i e^{-(D_s|\omega|^2+1/\tau)s} e^{2\pi i\omega\cdot\mathbf{x}}|\} ds$$
$$\leq 2\pi \int_0^{t_0} e^{-s/\tau} \sum_{\omega\in\mathbb{Z}^n} |\omega| e^{-D_s|\omega|^2 s} ds.$$

Using the fact $e^{-s/\tau} \leq 1$, and the Poisson summation formula, we have

$$I \leq 2\pi \int_0^{t_0} \left(\frac{\pi}{D_s s}\right)^{\frac{n}{2}+2} \sum_{\omega\in\mathbb{Z}^n} |\omega| e^{-\pi^2 \frac{|\omega|^2}{D_s s}} ds.$$

Using the fact that the summand is positive and bounded we can use Fubini–Tonelli theorem to interchange the sum and integral

$$= 2\pi \left(\frac{\pi}{D_s}\right)^{\frac{n}{2}+2} \sum_{\omega\in\mathbb{Z}^n:\, |\omega|\neq 0} |\omega| \int_0^{t_0} \left(\frac{1}{s}\right)^{\frac{n}{2}+2} e^{-\pi^2 \frac{|\omega|^2}{D_s s}} ds.$$

We can bound the integrand by taking its value at its maximum $s = \frac{2\pi|\omega|^2}{D_s(n+4)}$

$$\leq 2\pi \left(\frac{\pi}{D_s}\right)^{\frac{n}{2}+2} \left(\frac{D_s(n+4)}{2\pi^2}\right)^{\frac{n}{2}+2} e^{-\frac{(n+4)}{2}} \sum_{\omega\in\mathbb{Z}^n:\, |\omega|\neq 0} \frac{1}{|\omega|^{n+3}} \int_0^{t_0} ds$$
$$\leq 2\pi \left(\frac{n+4}{2\pi}\right)^{\frac{n}{2}+2} e^{-\frac{(n+4)}{2}} t_0 \sum_{\omega\in\mathbb{Z}^n:\, |\omega|\neq 0} \frac{1}{|\omega|^{n+3}}.$$

With the intention of bounding this sum by an integral consider the extension

$$\sum_{\omega\in\mathbb{Z}^n:\, |\omega|\neq 0} \frac{1}{|\omega|^{n+3}} \leq \sum_{\omega\in\mathbb{Z}^n} f(\omega),$$

where

$$f(\omega) = \begin{cases} 1 & if\ |\omega| \leq 1, \\ |\omega|^{-n-3} & otherwise. \end{cases}$$

Using a similar argument as before we can bound this sum by its integral over $\mathbb{R}^n$

$$\begin{aligned}\sum_{\omega\in\mathbb{Z}^n:\,|\omega|\neq 0}\frac{1}{|\omega|^{n+3}} &\leq \int_{\mathbb{R}^n} f(\omega)d\omega \\ &= \frac{2\pi^{\frac{n}{2}}}{\Gamma(\frac{n}{2})}\int_0^\infty |\omega|^{n-1}f(\omega)d|\omega| \\ &= \frac{2\pi^{\frac{n}{2}}}{\Gamma(\frac{n}{2})}\left(\int_0^1 |\omega|^{n-1}d|\omega| + \int_1^\infty \frac{1}{|\omega|^4}d|\omega|\right) \\ &= \frac{2\pi^{\frac{n}{2}}}{\Gamma(\frac{n}{2})}\left(\frac{3+n}{3n}\right).\end{aligned}$$

Substituting this bound back into I yields

$$I \leq 2\pi\left(\frac{n+4}{2\pi}\right)^{\frac{n}{2}+2} e^{-\frac{(n+4)}{2}}\frac{2\pi^{\frac{n}{2}}}{\Gamma(\frac{n}{2})}\left(\frac{3+n}{3n}\right)t_0 \tag{2.61}$$

$$\leq \frac{(n+4)^{\frac{n}{2}+2}}{2^{\frac{n}{2}}\pi\Gamma(\frac{n}{2})}\left(\frac{3+n}{3n}\right)t_0. \tag{2.62}$$

Putting this bound together with (2.59), we can bound $\|\nabla S\|_\infty$, again using $e^{-s/\tau}\leq 1$

$$\begin{aligned}\|\nabla S\|_\infty &\leq \alpha\|\rho_0\|_1\left(\frac{(n+4)^{\frac{n}{2}+2}}{2^{\frac{n}{2}}\pi\Gamma(\frac{n}{2})}\left(\frac{3+n}{3n}\right)t_0 + \int_{t_0}^t 8\pi^2\frac{\Gamma(\frac{n+1}{2})}{\Gamma(\frac{n}{2})}\left(\frac{1}{D_s s}\right)^{\frac{3}{2}}e^{-s/\tau}ds\right) \\ &\leq \alpha\|\rho_0\|_1\left(\frac{(n+4)^{\frac{n}{2}+2}}{2^{\frac{n}{2}}\pi\Gamma(\frac{n}{2})}\left(\frac{3+n}{3n}\right)t_0 + 8\pi^2\frac{\Gamma(\frac{n+1}{2})}{\Gamma(\frac{n}{2})}\int_{t_0}^t\left(\frac{1}{D_s s}\right)^{\frac{3}{2}}ds\right) \\ &\leq \alpha\|\rho_0\|_1\left(\frac{(n+4)^{\frac{n}{2}+2}}{2^{\frac{n}{2}}\pi\Gamma(\frac{n}{2})}\left(\frac{3+n}{3n}\right)t_0 + 8\pi^2\frac{\Gamma(\frac{n+1}{2})}{\Gamma(\frac{n}{2})}t_0^{-\frac{1}{2}}\right).\end{aligned}$$

Now, we maximize the inequality by taking t_0 at

$$t_0 = \left(\frac{12n\pi^3 2^{\frac{n}{2}}\Gamma(\frac{n+1}{2})}{(3+n)(n+4)^{\frac{n}{2}+2}e^{-\frac{(n+4)}{2}}}\right)^{\frac{2}{3}}, \tag{2.63}$$

inputting this value into our inequality yields

$$\|\nabla S\|_\infty \leq \alpha \frac{12}{2^{\frac{2}{3}}} \frac{c(n)}{D_s} \|\rho_0\|_{L^1(\mathbb{T}^n)}^{\frac{1}{2}}, \tag{2.64}$$

where

$$c(n) := \frac{(\Gamma(\frac{n+1}{2}))^{\frac{2}{3}}}{\Gamma(\frac{n}{2})} \left(\frac{(n+4)^{\frac{n}{2}+2}}{2^{\frac{n}{2}}} \left(\frac{3+n}{3n} \right) e^{-\frac{n+4}{2}} \right)^{\frac{1}{3}}, \tag{2.65}$$

which is the required bound. Although we have only shown the proof for the case where $\tau = \mathcal{O}(1)$, throughout the proof we used the bound $e^{-t/\tau} \leq 1$, which is still valid if we take $\tau = \infty$ $\square$

Remark 3 *It is difficult to see how small this bound really is due to the esoteric nature of $c(n)$. For dimensions $n = 2$, and $n = 3$ the constant is approximately $c(2) \approx 1.5$, and $c(3) \approx 4$.*

2.5 Theorem 2: Global existence

With these estimates on ∇S and ρ,

we can find a condition on the parameters such that the turning kernel is positive for all time.

Lemma 4 *If $(P_0 = \rho_0 q, S_0 = 0) \in \mathcal{X}$, T is continuous from this phase space $\mathcal{X}$ to $\mathbb{R}$ for each $(\boldsymbol{x}, \boldsymbol{v}) \in \mathbb{T}^n \times V$, and*

$$q(\boldsymbol{v}) > \alpha \frac{12c(n)}{2^{\frac{2}{3}} D_s} b(\boldsymbol{x}, \boldsymbol{v}) \|v\|_{L^\infty(V)} \|\rho_0\|_{L^1(\mathbb{T}^n)} \quad \forall\, (\boldsymbol{x}, \boldsymbol{v}) \in V \times \mathbb{T}^n, \tag{2.66}$$

then

$$T(x, \boldsymbol{v}, t) \geq 0, \quad \forall (x, \boldsymbol{v}, t) \in \mathbb{T}^n \times V \times \mathbb{R}_+. \tag{2.67}$$

Proof:
First, note that for $t = 0$ we have $T > 0$, by our choice of initial conditions. We define the time $t_1 := \sup_{t \in \mathbb{R}_+} \{T \geq 0, \quad \forall (\mathbf{x}, \mathbf{v}) \in \mathbb{T}^n \times V\} > 0$. We proceed

by contradiction, we assume that $t_1 < \infty$. At t_1, we have that

$$\begin{aligned} T &= q + b(1-\rho)\mathbf{v}\cdot\nabla S, \\ &\geq q - b|1-\rho|\|\mathbf{v}\|_{L^\infty(\mathbb{V})}\|\nabla S\|_{L^\infty(\mathbb{T}^n)}. \end{aligned} \tag{2.68}$$

Then, using the new $\|\nabla S\|$ inequality (2.48)

$$T \geq q - b|1-\rho|\|\mathbf{v}\|_{L^\infty(\mathbb{V})}\left(\alpha\frac{12}{2^{\frac{2}{3}}}\frac{c(n)}{D_s}\|\rho_0\|_{L^1(\mathbb{T}^n)}\right), \tag{2.69}$$

but

$$q(\mathbf{v}) > \alpha\frac{12c(n)}{2^{\frac{2}{3}}D_s}b(\mathbf{x},\mathbf{v})\|v\|_{L^\infty(V)}\|\rho_0\|_{L^1(\mathbb{T}^n)} \quad \forall\ (\mathbf{x},\mathbf{v}), \tag{2.70}$$

thus, $T > 0$, which implies t_1 is not the largest time for which $T \geq 0$ and is therefore a contradiction. A Similar argument can be made for $\tau = \infty$ $\square$

Now with this *Lemma*, we can extend the local existence of the kinetic-chemotaxis system to global existence.

Theorem 2 *Consider the model* (2.1) - (2.3)*, with the assumption* (2.66)*, the initial conditions* $(P_0 = \rho_0 q, S_0 = 0) \in \mathcal{X}$*, and* T *is continuous from this phase space* $\mathcal{X}$ *to* $\mathbb{R}$ *for each* $(\boldsymbol{x},\boldsymbol{v}) \in \mathbb{T}^n \times V$*, then the mild solution (P,S) exists globally:* $P \in C((0,\infty); L^2(\mathbb{T}^n \times V))$*,* $S \in C((0,\infty); C^\infty(\mathbb{T}^n))$

Proof:
Consider the equations

$$P_t + (\mathbf{v}\cdot\nabla)P = \mu(q + b(1-\rho)\mathbf{v}\cdot\nabla S)\rho - \mu P, \in \mathbb{T}^n \times V \times \mathbb{R}_+ \tag{2.71}$$

$$S_t - D_s\Delta S = \alpha\rho - \frac{1}{\tau}S, \in \mathbb{T}^n \times \mathbb{R}_+, \tag{2.72}$$

with initial conditions $(P_0 = \rho_0 q, S_0 = 0) \in \mathcal{X}$, and since T is continuous from this phase space $\mathcal{X}$ to $\mathbb{R}$ for each $(\mathbf{x},\mathbf{v}) \in \mathbb{T}^n \times V$, by Theorem 1 a solution (P, S) exists and is unique. Now, since

$$q(\mathbf{v}) > \alpha\frac{12c(n)}{2^{\frac{2}{3}}D_s}b(\mathbf{x},\mathbf{v})\|v\|_{L^\infty(V)}\|\rho_0\|_{L^1(\mathbb{T}^n)} \quad \forall\ (\mathbf{x},\mathbf{v}) \in V \times \mathbb{T}^n \tag{2.73}$$

Lemma 4 implies that the turning kernel is positive i.e $T[\rho, S](\mathbf{x},\mathbf{v},t) \geq 1$ for

all $(\mathbf{x}, \mathbf{v}, t) \in \mathbb{T}^n \times V \times \mathbb{R}_+$. Having the turning kernel be always positive means the *Lemmas* 1 through 3 apply.

Now, *Lemma* 1 bounds $P \leq q$, which gives us

$$\|P\|_{L^2(\mathbb{T}^n \times V)} = \int_{\mathbb{T}^n} \int_V |P|^2 d\mathbf{x} d\mathbf{v}, \tag{2.74}$$

$$\leq \int_{\mathbb{T}^n} \int_V |q(\mathbf{v})|^2 d\mathbf{x} d\mathbf{v} \tag{2.75}$$

$$= |\mathbb{T}^n| \|q\|_{L^2(V)} < \infty \tag{2.76}$$

by the initial conditions $\rho_0(\mathbf{x})q(\mathbf{v}) \in L^2(V) \times H^1(\mathbb{T}^n)$. Another consequence of *Lemma* 1 is $\rho \leq 1$ for all time which allows us to write down an explicit solution to S by *Lemma* 2

$$S(x,t) = \alpha \int_0^t \int_{\mathbb{T}^n} \rho(y,s) G(x-y, t-s) dy ds. \tag{2.77}$$

With the solution S taking this form, it is clear that its derivatives are bounded since the derivatives can be moved on the Green's function. Thus, for the equations(2.1) - (2.3), with the initial conditions $(P_0 = \rho_0 q, S_0 = 0) \in \mathcal{X}$, and assumptions on q,and T we find that, $(P, S) \in C((0,\infty); L^2(\mathbb{T}^n \times V)) \times C((0,\infty); C^\infty(\mathbb{T}^n))$ $\square$

Remark 4 *Note that we only have a bound on P in $L^2(\mathbb{T}^n \times V)$, thus, P is only in $C((0,\infty); L^2(\mathbb{T}^n \times V))$, instead of $C((0,\infty); \{\phi_P \in L^2(V \times \mathbb{T}^n) : \phi_P(\cdot, \boldsymbol{v}) \in H^1(\mathbb{T}^n)\})$.*

We are in the unusual position of having a mild solution for the kinetic equation, but a classical solution for the chemotactic equation. This situation occurs because we cannot define ∇P in the traditional sense, where in the solution to the chemotactic equation we can move derivatives onto the Green's function, which has bounded derivatives i.e. $\Delta S(\mathbf{x}, t) = \Delta(G * \rho)(\mathbf{x}, t) = (\rho * \Delta G)(\mathbf{x}, t)$. Now that our base model has global solutions, we can more safely move on to analyzing scaling limits, knowing we are not working on an empty set.

Chapter 3

Scaling Limits

The kinetic equation (2.1) is based on dynamics at the cellular level, but our goal is to examine population-level dynamics. It is reasonable to consider approximate solutions that relate to longer timescales and larger space scales, and while we are changing the scales, it is worth averaging out the velocity dependence.

The standard argument is to look at the size of the parameters. Consider the values for μ and characteristic speed, which can be enormous compared to the time scale of population dynamics. For example E. coli $\mu \approx 1/sec$, and $|\mathbf{v}| \approx 10^{-2} mm/sec$, but experiments occur on time scale of hours, days [40]. Switching units to $U = 10000\ sec \approx 3hrs$. Introducing $\epsilon := 10^{-2}$, So $\mu = \epsilon^{-2}\tilde{\mu}$, and $|\mathbf{v}| = \epsilon^{-1}|\tilde{\mathbf{v}}|$, then we can write (2.1)

$$\epsilon^2 P_t(\mathbf{x}, \mathbf{v}, t) + \epsilon \tilde{\mathbf{v}} \cdot \nabla_{\mathbf{x}} P(\mathbf{x}, \mathbf{v}, t) = -\tilde{\mu} P(\mathbf{x}, \mathbf{v}, t) + \tilde{\mu} \int_V T[S, \rho](\mathbf{x}, \mathbf{v}) P(\mathbf{x}, \mathbf{v}', t) d\mathbf{v}', \tag{3.1}$$

We gain the same result by rescaling space and time, namely by the parabolic scaling. There are two common scalings:

- previously mentioned, **parabolic scaling** $\tau = \epsilon^2 t$, and $\xi = \epsilon x$,
- **hyperbolic scaling** $\tau = \epsilon t$, and $\xi = \epsilon x$.

How do we choose between the scalings? This depends mostly on whether the system is **diffusion** dominated versus **advection** dominated. There are

other asymptotic scalings based on wave movement like $\xi = \epsilon^{\alpha}(\mathbf{x} - \mathbf{a}_0 t)$, $\tau = \epsilon^{\alpha+\beta} t$, that are used for small disturbances about the equilibrium state [52]. Another property of these approximations is that the equations are in terms of statistically significant quantities of the cell density P and the turning kernel T, like the expectation and variance. For this reason, we define the expectation of a scalar function $\phi \in L^2(V)$ to be

$$\mathbb{E}_\phi := \int_V \mathbf{v}\phi(\mathbf{v}) d\mathbf{v}, \tag{3.2}$$

and the variance to be

$$\mathbb{V}_\phi := \int_V (\mathbf{v} - \mathbb{E}_\phi)(\mathbf{v} - \mathbb{E}_\phi)^T \phi(\mathbf{v}) d\mathbf{v}. \tag{3.3}$$

This work will go over four different ways to arrive at a macroscopic model, the hyperbolic or hydrodynamic scaling, parabolic scaling, and two different moment closures methods. Each of these methods relies on a different approximation, meaning some methods will be more applicable to different biological scenarios. The two scalings have to do entirely with the size of the problem and the period the dynamics play over. The two different moment closures methods are based on approximating higher-order moments. In analyzing the methods, we gain generality, and it is interesting to analyze the differences that arise from the different methods.

It is important to note that we use these approximations only on the kinetic equation (2.1), especially in the case of the scalings. The chemoattractant equation (2.2) is assumed to be already on the macroscopic scale; therefore, it remains unchanged throughout the various scalings.

3.1 Parabolic Scaling

Parabolic systems' distinguishing feature is that there is no preferred direction, making diffusion the major dynamical player. The diffusion dynamics naturally occur at the new scaled coordinates $\tau = \epsilon^2 t$, $\xi = \epsilon x$, where $\epsilon << 1$, due to the scaling symmetry of parabolic equations. After transforming to the

new coordinates, (2.1) becomes

$$\epsilon^2 P_\tau + \epsilon \mathbf{v} \cdot \nabla_\xi P = \mu \left(q[\rho] + \epsilon b[S](1-\rho)\mathbf{v} \cdot \nabla S \right) \rho - \mu P. \tag{3.4}$$

To analyse the scaled equation (3.4), we take the scaled coordinates (ξ, τ) and make a regular expansion in ϵ, called a *Hilbert expansion* [12]

$$P(\tau, \xi, \mathbf{v}) = P_0(\tau, \xi, \mathbf{v}) + \epsilon P_1(\tau, \xi, \mathbf{v}) + \epsilon^2 P_2(\tau, \xi, \mathbf{v}) + \dots \tag{3.5}$$

A further assumption is that all of the mass is contained in the first order

$$\rho = \rho_0, \quad \int_V P_i d\mathbf{v} = 0, \ \ \forall i \geq 1. \tag{3.6}$$

Substituting the *Hilbert* expansions into the rescaled transport equation (3.4), and a comparison of terms equal order yields a countable number of equations at different orders ϵ that all must vanish independently. The zeroth-order is given by

$$P_0(\tau, \xi, \mathbf{v}) = q[\rho](\xi, \mathbf{v})\rho(\xi, t). \tag{3.7}$$

The next order of ϵ gives

$$\mathbf{v} \cdot \nabla P_0 - \mu(\mathbf{v} \cdot \nabla) b[S](1-\rho)\rho = \mu P_1. \tag{3.8}$$

Solving this equation in terms of P_1 leads to

$$P_1 = -\frac{1}{\mu} \left(\mathbf{v} \cdot \nabla P_0 - \mu(\mathbf{v} \cdot \nabla) b[S](1-\rho)\rho \right). \tag{3.9}$$

Finally, to get a closed system for the first term in the Hilbert expansion P_0, we look at the ϵ^2 terms

$$(P_0)_\tau + \mathbf{v} \cdot \nabla P_1 = -\mu P_2. \tag{3.10}$$

Integrating over V, the right-hand side vanishes and substituting P_1 yields an equation in terms of ρ

$$\rho_\tau - \frac{1}{\mu}\int_V \left((\mathbf{v}\cdot\nabla)\left((\mathbf{v}\cdot\nabla)(\rho q[\rho]) - (\mathbf{v}\cdot\nabla S)b[S](1-\rho)\rho\right)\right) d\mathbf{v} = 0, \quad (3.11)$$

simplifying in component form

$$\rho_\tau - \frac{1}{\mu}\partial_i\partial_j\left(\rho\int_V v_i v_j q[\rho] d\mathbf{v}\right) + \frac{1}{\mu}\partial_i\left(\partial_j(S)\rho(1-\rho)\int_V v_i v_j b[S] d\mathbf{v}\right) = 0, \quad (3.12)$$

repeated indices are summed from 1 to n. Using the previously defined expectation (3.20) and variance tensors (3.3), we can write the above equation in a more compact form with the identity

$$\begin{aligned}
\mathbb{V}_q &= \int_V (\mathbf{v}-\mathbb{E}_q)(\mathbf{v}-\mathbb{E}_q)^T q d\mathbf{v} && (3.13)\\
&= \int_V \mathbf{v}\mathbf{v}^T q d\mathbf{v} - 2\int_V \mathbf{v}\mathbb{E}_q^T q d\mathbf{v} + \int_V \mathbb{E}_q\mathbb{E}_q^T q d\mathbf{v} && (3.14)\\
&= \int_V \mathbf{v}\mathbf{v}^T q d\mathbf{v} - \int_V \mathbb{E}_q\mathbb{E}_q^T \hat{P} d\mathbf{v}, && (3.15)
\end{aligned}$$

and the accompanying chemoattractant equation

$$\begin{aligned}
&\rho_\tau - \frac{1}{\mu}\nabla\left(\nabla\left(\mathbb{V}_q[\rho]\rho + \mathbb{E}_q[\rho]\mathbb{E}_q[\rho]^T\rho\right) - \rho(1-\rho)\mathbb{V}_b[S]\nabla S\right) = 0,\\
&S_\tau - D_s\Delta S = \alpha\rho - \frac{1}{\tau}S.
\end{aligned} \quad (3.16)$$

Note that this appears to be a more general system of the Keller-Segel equations [35], with the inclusion of the anisotropy of $\mathbb{V}_q + \mathbb{E}_q\mathbb{E}_q^T$, and $\mathbb{V}_b$. The effect of the $\mathbb{V}_q$, and $\mathbb{V}_b$ terms are nonuniform diffusion, and mixing of the ∇S into other directions. Of course the above scenarios are dependent on the given distributions $q[\rho](\mathbf{x},\mathbf{v})$, and $b[S](\mathbf{x},\mathbf{v})$. For instance, if q and b are uniform distributions in $\mathbf{v}$ neither nonuniform diffusion, nor mixing will occur. To further explore the effects of anisotropy, we will bring back the example

from Chapter one (1.8), and (1.9)

$$q(\mathbf{x},\mathbf{v}) = c(\mathbf{x})\left(e^{k\mathbf{v}\cdot\mathbf{u}} + e^{-k\mathbf{v}\cdot\mathbf{u}}\right), \quad b = \beta(\mathbf{x}) + \mathbf{v}^T A(\mathbf{x})\mathbf{v},$$

calculating the quantities $\mathbb{V}_q$, and $\mathbb{V}_b$. For $\mathbb{V}_q$, in component form we have

$$(\mathbb{V}_q)_{ij} = c(\mathbf{x})\int_V \left(e^{k\mathbf{v}\cdot\mathbf{u}} + e^{-k\mathbf{v}\cdot\mathbf{u}}\right) v_i v_j d\mathbf{v}.$$

In the case of two dimensions, we have the following formula [30]

$$\mathbb{V}_q = \frac{1}{2}\left(1 - \frac{I_2(k)}{I_0(k)}\right)\mathbb{I} + \frac{I_2(k)}{I_0(k)}\mathbf{u}\mathbf{u}^T, \tag{3.17}$$

and

$$\mathbb{E}_q = 0. \tag{3.18}$$

For example take the fibre direction to be $\mathbf{u} = (\frac{1}{\sqrt{2}}, \frac{1}{\sqrt{2}})$, then

$$\mathbb{V}_q = \frac{1}{2}\mathbb{I} + \frac{1}{2}\frac{I_2(k)}{I_0(k)}\begin{pmatrix} 0 & 1 \\ 1 & 0 \end{pmatrix}. \tag{3.19}$$

The second term causes diffusion to be increased along the directions $(\frac{1}{\sqrt{2}}, \frac{1}{\sqrt{2}})$ and $(-\frac{1}{\sqrt{2}}, -\frac{1}{\sqrt{2}})$. The strength of the anisotropy is based on the concentration parameter k, where limiting cases are $\frac{I_2(k)}{I_0(k)} \to 0$ as $k \to 0$, making the diffusion tensor isotropic, and the case $\frac{I_2(k)}{I_0(k)} \to 1$ as $k \to \infty$, making the diffusion tensor to be maximally anisotropic.

Now for $\mathbb{V}_b$ in component form we have

$$(\mathbb{V}_b)_{i_1\, i_2} = \int_V \left(\beta(\mathbf{x}) + A_{i_3\, i_4} v_{i_3} v_{i_4}\right) v_{i_1} v_{i_2} d\mathbf{v},$$

moving the constants out of the integrals, and defining mean velocity tensor to be

$$\bar{v}^{i_1,\ldots,i_k} := \int_V v_{i_1}\cdots v_{i_k} d\mathbf{v}, \tag{3.20}$$

we can rewrite

$$(\mathbb{V}_b)_{i_1\, i_2} = \beta(\mathbf{x})\bar{v}^{i_1\, i_2} + A_{i_3\, i_4}\bar{v}^{i_1\, i_2\, i_3\, i_4},$$

using the *Lemma* 2.2 from [25], we can explicitly compute the $\bar{v}$'s from (3.20)

$$(\mathbb{V}_b)_{i_1\, i_2} = \frac{|\mathbb{S}^{n-1}|}{n}\left(2\beta(\mathbf{x})\mathbb{I}_{i_1\, i_2} + \frac{s^{3-n}}{n+2}A_{i_1\, i_2}\sum_{\mathcal{P}(i_1\, i_2\, i_3\, i_4)}\delta_{i_{j_2}}^{i_{j_1}}\delta_{i_{j_4}}^{i_{j_3}}\right), \tag{3.21}$$

where the set of pairs of indices out of $(i_1, \ldots, i_4)$ is defined as

$$\mathcal{P}(i_1\, i_2\, i_3\, i_4) := \{((i_{j_1}, i_{J_2})(i_{j_3}, i_{j_4})) : j_1, j_2, j_3, j_4 = 1, 2, 3, 4\}. \tag{3.22}$$

We can compute the sum explicitly since there is only 12 combinations and to the symmetry of the Kronecker delta where there are only 3 unique terms

$$(\mathbb{V}_b)_{i_1\, i_2} = \frac{|\mathbb{S}^{n-1}|}{n}\left(2\beta(\mathbf{x})\mathbb{I}_{i_1\, i_2} + \frac{4s^{3-n}}{n+2}A_{i_1\, i_2}(\delta_{i_2}^{i_1}\delta_{i_4}^{i_3} + \delta_{i_3}^{i_1}\delta_{i_4}^{i_2} + \delta_{i_3}^{i_2}\delta_{i_4}^{i_1})\right). \tag{3.23}$$

Using the properties of the Kronecker delta, we can convert back to matrix notation

$$\mathbb{V}_b = \frac{|\mathbb{S}^{n-1}|}{n}\left(2\beta(\mathbf{x})\mathbb{I} + \frac{4s^{3-n}}{n+2}(Tr(A)\mathbb{I} + A + A^T)\right). \tag{3.24}$$

As a result, we have anisotropic component caused by the off-diagonal pieces of A. If A has nonzero off-diagonal components, then $\mathbb{V}_b$ has a mixing effect on the chemotactic velocity

$$u(\mathbf{x}, t) := \mathbb{V}_b \nabla S.$$

To see this, consider the two dimensional case

$$u_i(\mathbf{x}, t) := \left(\mathbb{V}_b^{i,1}\partial_x S + \mathbb{V}_b^{i,2}\partial_y S\right), \quad i = \{1, 2\},$$

the velocity in the x direction is dependent on the chemotactic gradient in the y direction, and vice versa. In summary, the new terms create non-uniform diffusion and mixing of influence of the chemotactic gradient. The effect of the chemotactic mixing will be shown through numerics in Chapter 4. Next, we will look at the rigorous parabolic limit where we take $\epsilon \to 0$ in (3.4).

3.1.1 Rigorous Parabolic Limit

Now, it is questionable whether the kinetic chemotaxis system (3.1) converges to this Keller-Segel type equation (3.16) in the limit as ϵ goes to zero, and in what sense. Again, for this section we will limit ourselves to the case where $q := q(\mathbf{v})$, and $b := b(\mathbf{x}, \mathbf{v})$. To compute the parabolic limit, we need *a priori* estimates on P, S that are uniform in ϵ. Since the chemoattractant equation is unchanged in the parabolic case, *Lemma* 3 is available. With the same idea of using positivity to gain L^∞ bounds on P.

Lemma 5 *If (S,P) are solutions to* (2.1) - (2.3) *as in Theorem 1,* $P_0(\boldsymbol{x}, \boldsymbol{v}) = q(\boldsymbol{v})\rho_0(\boldsymbol{x})$*, and* $T_\epsilon[\rho, S](\boldsymbol{x}, \boldsymbol{v}) \geq 0, \quad \forall(\boldsymbol{x}, \boldsymbol{v}, t) \in \mathbb{T}^n \times V \times [0, t_*]$*, then*

$$P(\boldsymbol{x}, \boldsymbol{v}, t) \leq q(\boldsymbol{v}), \quad \rho(\boldsymbol{x}, t) \leq 1, \quad \forall(\boldsymbol{x}, \boldsymbol{v}, t) \in \mathbb{T}^n \times V \times [0, t_*]. \tag{3.25}$$

Proof:
Consider the transformation

$$\tilde{P} = q - P, \quad \tilde{\rho} = \int_V \tilde{P} d\mathbf{v} = 1 - \rho, \tag{3.26}$$

$$\tilde{S} = \alpha\tau - S. \tag{3.27}$$

Substituting this change of variables into the kinetic-chemotaxis system (3.4)

$$\epsilon^2(q - \tilde{P})_t + \epsilon\mathbf{v} \cdot \nabla(q - \tilde{P}) = \mu\left((q - \epsilon b\tilde{\rho}\mathbf{v} \cdot \nabla\tilde{S})(1 - \tilde{\rho}) - (q - \tilde{P})\right), \tag{3.28}$$

$$-\epsilon^2\tilde{P}_t - \epsilon\mathbf{v} \cdot \nabla\tilde{P} = -\mu\left((q\tilde{\rho} - \epsilon b(1 - \tilde{\rho})\tilde{\rho}\mathbf{v} \cdot \nabla\tilde{S}) - \tilde{P})\right), \tag{3.29}$$

$$\epsilon^2\tilde{P}_t + \epsilon\mathbf{v} \cdot \nabla\tilde{P} = \mu\left((q\tilde{\rho} - \epsilon b(1 - \tilde{\rho})\tilde{\rho}\mathbf{v} \cdot \nabla\tilde{S}) - \tilde{P})\right), \tag{3.30}$$

which is the same as the scaled kinetic equation (3.4). Now it is clear that the kinetic equation is invariant under translation by q. Thus, the rest of the proof follows from the arguments in *Lemma* 1. □

With the above *Lemma*, we have both of the *a priori* estimates on P and S needed to establish convergence.

Theorem 3 *Consider the model* (2.1) - (2.3)*, with the assumption* (2.66)*, the initial conditions* $(P_0 = \rho_0 q, S_0 = 0) \in \mathcal{X}$*, and* T *is continuous from this phase space* $\mathcal{X}$ *to* $\mathbb{R}$ *for each* $(\boldsymbol{x}, \boldsymbol{v}) \in \mathbb{T}^n \times V$*,*
then as $\epsilon \to 0$*, there is a weak limit*

$$P_\epsilon \rightharpoonup \rho q, \quad S_\epsilon \rightharpoonup S, \tag{3.31}$$

where (P_ϵ, S_ϵ) *satisfy the rescaled kinetic equation*

$$\epsilon^2 (P_\epsilon)_t + \epsilon v \cdot \nabla P_\epsilon = \mu(T_\epsilon[\rho_\epsilon, S_\epsilon]\rho_\epsilon - P_\epsilon), \tag{3.32a}$$

$$(S_\epsilon)_t - D_s \Delta S_\epsilon = \alpha \rho_\epsilon - \frac{1}{\tau} S_\epsilon, \tag{3.32b}$$

$$P_\epsilon(x, v, 0) = P_0(x, v), \quad S_\epsilon(x, 0) = S_0(x), \tag{3.32c}$$

and (ρ, S) *satisfy in the distributional sense*

$$\begin{aligned} &\rho_\tau - \frac{1}{\mu} \nabla \left(\nabla \left(\mathbb{V}_q \rho + \mathbb{E}_q \mathbb{E}_q^T \rho \right) - \rho(1-\rho) \mathbb{V}_b \nabla S \right) = 0, \\ &S_t - D_s \Delta S = \alpha \rho - \frac{1}{\tau} S, \\ &\rho(x, 0) = \int_V P_0 dv, \quad S(x, 0) = S_0. \end{aligned} \tag{3.33}$$

Proof
The idea for the this proof is to use the L^2 bounds from the previous *Lemmas*, to provide uniform in ϵ bounds for the sequences P_ϵ, and S_ϵ, such that we can take convergent subsequences due to the weak compactness of reflexive Banach spaces [14]. Since for every $\epsilon > 0$ (P_ϵ, S_ϵ), satisfy (3.32a) and the *Lemmas* 3, and 5, we have the bounds

$$\|P_\epsilon\|^2_{L^2(\mathbb{T}^n \times V)} \leq C(|\mathbb{T}^n \times V|) \|P_0\|^2_{L^2(\mathbb{T}^n \times V)}, \quad \|\nabla S_\epsilon\|^2_{L^2(\mathbb{T}^n)} \leq c(n) \|\rho_0\|_{L^1(\mathbb{T}^n)}. \tag{3.34}$$

Now, we have L^2 bounds for both P_ϵ and ∇S_ϵ, all that is left to show is that $P_\epsilon \rightharpoonup q\rho$ and that we can choose a subsequence such that (3.33) is satisfied, at least in a distributional sense.

To this end, consider the $L^2(\mathbb{T}^n \times V \times [0,T])$ inner product of the rescaled transport equation (3.32a) and a test function $\psi \in C_c^\infty(\mathbb{T}^n \times V \times [0,T])$

$$\epsilon^2\langle\psi, (P_\epsilon)_t\rangle + \epsilon\langle\psi, (\mathbf{v}\cdot\nabla)P_\epsilon\rangle = \mu\langle\psi, (T[\rho_\epsilon, S_\epsilon]\rho_\epsilon - P_\epsilon)\rangle, \tag{3.35}$$

moving the derivatives on to the test function,

$$-\epsilon^2\langle\psi_t, P_\epsilon\rangle - \epsilon\langle(\mathbf{v}\cdot\nabla)\psi, P_\epsilon\rangle = \mu\langle\psi, (T[\rho_\epsilon, S_\epsilon]\rho_\epsilon - P_\epsilon)\rangle. \tag{3.36}$$

Due to the bounds (3.34), the inner products on the left-hand side are uniformly bounded in ϵ. Thus, when we pass the convergent subsequence through this equation, the left-hand side vanishes, leaving

$$\langle\psi, (q\rho - P)\rangle = 0. \tag{3.37}$$

Using the fact $C_c^\infty(\mathbb{T}^n \times V \times [0,T])$ is dense in $L^2(\mathbb{T}^n \times V \times [0,T])$, we have that

$$q\rho - P = 0 \;\; a.e. \;\; \mathbb{T}^n \times V. \tag{3.38}$$

We need to show that we can pick a subsequence that satisfies (3.33) in a distributional sense. For this reason, consider the rescaled kinetic equation integrated over the velocity space,

$$(\rho_\epsilon)_t + \nabla\cdot\int_V \frac{\mathbf{v}}{\epsilon}P_\epsilon d\mathbf{v} = 0, \tag{3.39}$$

defining the flow of the population density to be

$$J_\epsilon := \int_V \frac{\mathbf{v}}{\epsilon}P_\epsilon d\mathbf{v}. \tag{3.40}$$

Now we want to show that for $\phi \in C_c^\infty(\mathbb{T}^n \times [0,T])$, as $\epsilon_l \to 0$

$$\langle\nabla\cdot J_{\epsilon_l}, \phi\rangle \rightharpoonup \langle\nabla\cdot J, \phi\rangle := \langle -\frac{1}{\mu}\nabla\nabla : (\mathbb{V}_q\rho + \mathbb{E}_q\mathbb{E}_q^T\rho) + \nabla(\nabla S\mathbb{V}_b\rho(1-\rho)), \phi\rangle. \tag{3.41}$$

The first step to this goal is to rewrite J_ϵ, to recover the terms on the right-hand side. To do this, we solve (3.32a) in terms of P_ϵ and substitute into

J_ϵ

$$\begin{aligned} J_\epsilon &= \int_V \frac{\mathbf{v}}{\epsilon}(T_\epsilon[\rho_\epsilon, S_\epsilon]\rho_\epsilon - \frac{\epsilon^2}{\mu}(P_\epsilon)_t - \frac{\epsilon}{\mu}(\mathbf{v}\cdot\nabla)P_\epsilon)d\mathbf{v} \\ &= \int_V \frac{\mathbf{v}}{\epsilon}(q + \epsilon b(1-\rho_\epsilon)\mathbf{v}\cdot\nabla S_\epsilon)\rho_\epsilon d\mathbf{v} - \frac{\epsilon^2}{\mu}(J_\epsilon)_t - \frac{1}{\mu}\nabla\cdot\int_V \mathbf{v}\mathbf{v}^T P_\epsilon d\mathbf{v} \\ &= \mathbb{V}_b\nabla S_\epsilon(1-\rho_\epsilon)\rho_\epsilon - \frac{\epsilon^2}{\mu}(J_\epsilon)_t - \frac{1}{\mu}\nabla\cdot\int_V \mathbf{v}\mathbf{v}^T q\rho_\epsilon d\mathbf{v} - \frac{1}{\mu}\nabla\cdot\int_V \mathbf{v}\mathbf{v}^T(P_\epsilon - q\rho_\epsilon)d\mathbf{v}. \end{aligned} \tag{3.42}$$

Now that we have something resembling the equation we want, we substitute J_ϵ back into (3.39) and considering its $L^2(\mathbb{T}^n \times [0,T])$ inner product with ϕ

$$\begin{aligned} \langle(\rho_\epsilon)_t, \phi\rangle - \frac{1}{\mu}\langle\nabla\nabla : (\mathbb{V}_q\rho_\epsilon + \mathbb{E}_q\mathbb{E}_q^T\rho_\epsilon), \phi\rangle + \langle\nabla\cdot\mathbb{V}_b(1-\rho_\epsilon)\nabla S_\epsilon\rho_\epsilon, \phi\rangle \\ = \frac{\epsilon^2}{\mu}\langle\nabla\cdot(J_\epsilon)_t, \phi\rangle - \frac{1}{\mu}\langle\nabla\nabla : \int_V \mathbf{v}\mathbf{v}^T(P_\epsilon - q\rho_\epsilon)d\mathbf{v}, \phi\rangle. \end{aligned} \tag{3.43}$$

moving the derivatives onto ϕ

$$\begin{aligned} -\langle\rho_\epsilon, \phi_t\rangle - \frac{1}{\mu}\langle\mathbb{V}_q\rho_\epsilon, \nabla\nabla\phi\rangle - \langle\mathbb{V}_b(1-\rho_\epsilon)\nabla S_\epsilon\rho_\epsilon, \nabla\phi\rangle \\ = \frac{\epsilon^2}{\mu}\langle J_\epsilon, \nabla\phi_t\rangle - \frac{1}{\mu}\langle\int_V \mathbf{v}\mathbf{v}^T(P_\epsilon - q\rho_\epsilon)dv, \nabla\nabla\phi\rangle. \end{aligned} \tag{3.44}$$

All the terms are accounted for in the limit $\epsilon_l \to 0$, except for $\frac{\epsilon^2}{\mu}\langle J_\epsilon, \nabla\phi_t\rangle$. For the $\frac{\epsilon^2}{\mu}\langle J_\epsilon, \nabla\phi_t\rangle$ term, we can show that it is $\mathcal{O}(\epsilon)$

$$\begin{aligned} \frac{\epsilon^2}{\mu}\int_0^T\int_{\mathbb{T}^n} J_\epsilon\phi_t dx ds &= \frac{\epsilon^2}{\mu}\int_0^T\int_{\mathbb{T}^n}\int_V \frac{\mathbf{v}P_\epsilon}{\epsilon}d\mathbf{v}\phi_t d\mathbf{x}ds \\ &\le \frac{\epsilon}{\mu}\int_0^T \|\phi_t\|_{L^\infty(\mathbb{T}^n)}\|\int_V \mathbf{v}P_\epsilon d\mathbf{v}\|_{L^1(\mathbb{T}^n)}dt \\ &\le \frac{\epsilon}{\mu}\int_0^T \|\phi_t\|_{L^\infty(\mathbb{T}^n)}\|\mathbf{v}P_\epsilon\|_{L^1(\mathbb{T}^n\times V)}dt \\ &\le \frac{\epsilon}{\mu}\|\mathbf{v}\|_{L^\infty(V)}\|P_0\|_{L^1(\mathbb{T}^n\times V)}\int_0^T \|\phi_t\|_{L^\infty(\mathbb{T}^n)}dt, \end{aligned} \tag{3.45}$$

Now, finally we can take the limit

$$-\langle \rho, \phi_t \rangle - \frac{1}{\mu}\langle \mathbb{V}_q \rho + \mathbb{E}_q \mathbb{E}_q^T, \nabla\nabla\phi \rangle - \langle \mathbb{V}_b \nabla S(1-\rho)\rho, \nabla\phi \rangle = 0, \tag{3.46}$$

as required. □

The parabolic scaling is the most used of the various approximating methods for the kinetic equation in biology. The choice of parabolic scaling is due to the parameters of the kinetic equation being on the time scale of the individuals rather than the timescale of observation and this difference tends to be many orders of magnitude. In addition, the size between the average speed and the turning rate is huge. Through our parabolic scaling, we obtained a result that is similar to the classical Keller-Segel equation, except for the nonuniform diffusion and mixing of chemotactic velocities. The above Theorem (3) shows that limit sending $\epsilon \to 0$ takes solutions of the parabolic rescaled kinetic equation (3.4) to the Keller-Segel like equation (3.16) in the distributional sense. Next, we look at a macroscopic time and space scale where the average speed and turning rate are of the same order of magnitude.

3.2 Hyperbolic Scaling

The hyperbolic limit is a specific asymptotic expansion where the time and space scales are the same. In this scheme, advective effects dominate over diffusive. Thus, we introduce hyperbolic scaling $\tau = \epsilon t$, $\xi = \epsilon x$, where $\epsilon << 1$, transport equation (2.1) becomes

$$\epsilon P_\tau + \epsilon \mathbf{v} \cdot \nabla_\xi P = \mu \left(\rho(q[\rho] + \epsilon(1-\rho) b[S] \mathbf{v} \cdot \nabla_\xi S) - P \right). \tag{3.47}$$

To analyse the scaled equation, we take the scaled coordinates (ξ, τ) and make a regular expansion in ϵ

$$P(\tau, \xi, \mathbf{v}) = P_0(\tau, \xi, \mathbf{v}) + \epsilon P_1(\tau, \xi, \mathbf{v}) + \epsilon^2 P_2(\tau, \xi, \mathbf{v}) + \dots \tag{3.48}$$

Again we assume that all the mass of P is contained in ρ_0

$$\rho = \rho_0, \quad \int_V P_i d\mathbf{v} = 0, \ \ \forall i \geq 1. \tag{3.49}$$

We now assume that each order of ϵ vanishes independently, so we are left with a countable infinite set of equations. Starting at the bottom, consider the zeroth order of ϵ, which is given by the q fibre distribution

$$P_0 = q[\rho]\rho. \tag{3.50}$$

On to the next order, we have

$$(P_0)_\tau + (\mathbf{v} \cdot \nabla)P_0 = -\mu P_1 + \mu\rho(1-\rho)b[S]\mathbf{v} \cdot \nabla S. \tag{3.51}$$

Now we can close the system by integrating $\mathbf{v}$ over V

$$\int_V (P_0)_\tau + (\mathbf{v} \cdot \nabla)P_0 d\mathbf{v} = -\mu \int_V P_1 d\mathbf{v} + \mu\rho(1-\rho)\nabla S \cdot \int_V b[S]\mathbf{v} d\mathbf{v}. \tag{3.52}$$

Then using the previous order condition (3.50), the assumptions on ρ_1 (3.49), and the assumption that all odd moments of b vanish (1.7), we arrive at the closed system

$$\rho_\tau + \nabla(\mathbb{E}_q \rho) = 0. \tag{3.53}$$

The above system is a closed system for the particle density ρ, and its dynamics are determined completely by the environmental fibres $q[\rho]$ through the mean movement direction $\mathbb{E}_q$. In a sense, this means that dispersion is, in essence, controlled by directions given by $q[\rho]$, but the chemotaxis term no longer arises. Hence, to understand the role of chemotaxis, we need to consider higher-order corrections. These corrections would dominate in cases when $\mathbb{E}_q = 0$, which occurs anywhere $q[\rho]$ is symmetric in V.

We can derive higher-order approximations by looking at the next order in

ϵ. Now consider first order in ϵ again (3.51), this time rearranged for P_1,

$$\begin{aligned} P_1 &= -\frac{1}{\mu}\left[(P_0)_\tau + (\mathbf{v}\cdot\nabla)P_0 - \mu\rho(1-\rho)b[S,\rho]\mathbf{v}\cdot\nabla S\right] \\ &= -\frac{1}{\mu}\left[(q[\rho]\rho)_\tau + (\mathbf{v}\cdot\nabla)(q[\rho]\rho) - \mu\rho(1-\rho)b[S,]\mathbf{v}\cdot\nabla S\right]. \end{aligned} \tag{3.54}$$

To obtain a next order correction term, we continue into second order in ϵ and we see a pattern begin to emerge

$$\begin{aligned} P_2 &= -\frac{1}{\mu}\left[(P_1)_\tau + (\mathbf{v}\cdot\nabla)P_1\right] \\ &= -\frac{1}{\mu}\left[(\partial_\tau + (\mathbf{v}\cdot\nabla))(-\frac{1}{\mu}\left[(q[\rho]\rho)_\tau + (\mathbf{v}\cdot\nabla)(q[\rho]\rho) - \mu\rho(1-\rho)b[S]\mathbf{v}\cdot\nabla S\right])\right]. \end{aligned} \tag{3.55}$$

By defining the advection opertator $\mathcal{W}_\mathbf{v} = \partial_\tau + (\mathbf{v}\cdot\nabla)$, we can greatly simplify the above expression. We then rewrite the ϵ^2 power as

$$P_2 = \left(-\frac{1}{\mu}\right)^2 \mathcal{W}_\mathbf{v}^2(q[\rho]\rho) - \frac{1}{\mu}\mathcal{W}_\mathbf{v}(\rho(1-\rho)b[S]\mathbf{v}\cdot\nabla S). \tag{3.56}$$

By looking at higher-order terms, it becomes clear that this pattern occurs at every order. To see this consider a short induction proof. First assume the form of P_k

$$P_k = \left(-\frac{1}{\mu}\right)^{k-1}\left[\mathcal{W}_\mathbf{v}^{k-1}(\rho(1-\rho)b[S]\mathbf{v}\cdot\nabla S) - \frac{1}{\mu}\mathcal{W}_\mathbf{v}^k(q[\rho]\rho)\right], \tag{3.57}$$

now consider the expression for P_{k+1}, from the ϵ^{k+1} power

$$\begin{aligned}
P_{k+1} &= -\frac{1}{\mu}\left[(P_k)_\tau + (\mathbf{v}\cdot\nabla)P_k\right] \\
&= -\frac{1}{\mu}\mathcal{W}_{\mathbf{v}}P_k \\
&= -\frac{1}{\mu}\mathcal{W}_{\mathbf{v}}\left(-\frac{1}{\mu}\right)^{k-1}\left[\mathcal{W}_{\mathbf{v}}^{k-1}(\rho(1-\rho)b[S]\mathbf{v}\cdot\nabla S) - \frac{1}{\mu}\mathcal{W}_{\mathbf{v}}^{k}(q[\rho]\rho)\right] \\
&= \left(-\frac{1}{\mu}\right)^{k}\left[\mathcal{W}_{\mathbf{v}}^{k}(\rho(1-\rho)b[S]\mathbf{v}\cdot\nabla S) - \frac{1}{\mu}\mathcal{W}_{\mathbf{v}}^{k+1}(q[\rho]\rho)\right].
\end{aligned}$$

Substituting this back into the Hilbert expansion for P, we obtain an asymptotic solution to the hyperbolic scaled transport equation

$$P = q[\rho]\rho + \sum_{k=1}^{\infty}(-1)^k\left(\frac{\epsilon}{\mu}\right)^k\left[\mathcal{W}_{\mathbf{v}}^{k}(q[\rho]\rho) - \mu\mathcal{W}_{\mathbf{v}}^{k-1}(\rho(1-\rho)b[S]\mathbf{v}\cdot\nabla S)\right]. \tag{3.58}$$

Now we can produce ϵ^k corrections by truncating the above sum. First, we insert the expansion (3.48) into the transport equation (3.47) then integrating over V

$$\rho_\tau + \int_V(\mathbf{v}\cdot\nabla)(P_0 + \epsilon P_1 + \epsilon^2 P_2 + \dots)dv = 0, \tag{3.59}$$

substituting (3.57) into the above equation yields

$$\begin{aligned}
&\rho_\tau + \int_V(\mathbf{v}\cdot\nabla)q[\rho]\rho d\mathbf{v} \\
&+ \int_V\left(\sum_{k=1}^{\infty}(-1)^k\left(\frac{\epsilon}{\mu}\right)^k\left[\mathcal{W}_{\mathbf{v}}^{k}(q[\rho]\rho) - \mu\mathcal{W}_{\mathbf{v}}^{k-1}(\rho(1-\rho)b[S]\mathbf{v}\cdot\nabla S)\right]\right)dv = 0.
\end{aligned} \tag{3.60}$$

For example, if we take on the first term of the sum, we arrive at the first-order correction

$$\rho_\tau + \nabla(\mathbb{E}_q[\rho]\rho) - \left(\frac{\epsilon}{\mu}\right)\int_V((\mathbf{v}\cdot\nabla)([\mathcal{W}_{\mathbf{v}}(q[\rho]\rho) - \mu\rho(1-\rho)b[S]\mathbf{v}\cdot\nabla S])dv + \mathcal{O}(\epsilon^2) = 0,$$

expanding $\mathcal{W}_{\mathbf{v}}$, we get

$$\rho_\tau + \nabla(\mathbb{E}_q[\rho]\rho) - \left(\frac{\epsilon}{\mu}\right)\int_V((\mathbf{v}\cdot\nabla)([(\partial_\tau + (\mathbf{v}\cdot\nabla))(q[\rho]\rho) - \mu\rho(1-\rho)b[S]\mathbf{v}\cdot\nabla S])dv + \mathcal{O}(\epsilon^2) = 0,$$

carrying out the operations, we obtain

$$\begin{aligned}\rho_\tau + \nabla(\mathbb{E}_q[\rho]\rho) - \left(\frac{\epsilon}{\mu}\right)\left[\nabla\nabla : \left(\int_V \mathbf{v}\mathbf{v}^T q[\rho]d\mathbf{v}\rho\right) + (\nabla(\mathbb{E}_q[\rho]\rho))_\tau\right] \\ + \epsilon\nabla\nabla S : (\rho(1-\rho)\mathbb{V}_b[S]) + \mathcal{O}(\epsilon^2) = 0.\end{aligned} \tag{3.61}$$

Using the fact that $\rho_\tau \approx -\nabla(\mathbb{E}_q\rho)$ up to order ϵ, we can write

$$\nabla(\mathbb{E}_q[\rho]\rho))_\tau = \nabla((\mathbb{E}_q[\rho])_\tau\rho + \mathbb{E}_q[\rho]\rho_\tau))) = -\nabla(((\mathbb{E}_q[\rho])_\rho\rho + \mathbb{E}_q)\nabla(\mathbb{E}_q[\rho]\rho)) + \mathcal{O}(\epsilon). \tag{3.62}$$

Therefore, we can write the second-order correction as

$$\begin{aligned}\rho_\tau + \nabla\cdot(\mathbb{E}_q[\rho]\rho) - \left(\frac{\epsilon}{\mu}\right)\left[\nabla\nabla : \left((\mathbb{V}_q[\rho] + \mathbb{E}_q[\rho]\mathbb{E}_q[\rho]^T)\rho\right)\right] \\ - \left(\frac{\epsilon}{\mu}\right)\nabla(((\mathbb{E}_q[\rho])_\rho\rho + \mathbb{E}_q[\rho])\nabla(\mathbb{E}_q[\rho]\rho)) + \epsilon\nabla\nabla S : (\rho(1-\rho)\mathbb{V}_b[S]) \approx 0.\end{aligned} \tag{3.63}$$

From here, we can see that if $q[\rho]$ is indeed symmetric in V, we will arrive at an equation resembling the parabolic scaling. Like many models derived from the kinetic equation, determining which scaling is a better approximation is whether or not $\mathbb{E}_q = 0$. Symmetry in q happens to be a case for most biological examples of $q[\rho]$ since $q[\rho]$ tends to be some sort of fibre distribution movement that is promoted along with both directions of the fibre.

Although there is an important example that breaks this paradigm, if we

assume that $b = \mathcal{O}(\epsilon^{-1})$, and again look at the first-order correction, we have

$$\rho_\tau + \nabla(\mathbb{E}_T[S,\rho]\rho)$$
$$+ \left(\frac{\epsilon}{\mu}\right)\left[\nabla\nabla : \left((\mathbb{V}_q + \mathbb{E}_q\mathbb{E}_q^T)\rho\right) - \nabla(\mathbb{E}_T[S,\rho]\nabla(\mathbb{E}_T[S,\rho]\rho)) + \nabla((\mathbb{E}_T[S,\rho])_\tau\rho)\right] \approx 0, \tag{3.64}$$

where

$$\mathbb{E}_T[S,\rho] := \mathbb{E}_q[\rho] + (1-\rho)\mathbb{V}_b[S]\nabla S. \tag{3.65}$$

We arrive at this equation through a nearly identical process to the previous hyperbolic scaling; thus, it is omitted for brevity. We obtain a very similar solution as the previous example

$$p = \sum_{k=0}^{\infty}(-1)^k\left(\frac{\epsilon}{\mu}\right)^k \mathcal{W}_{\mathbf{v}}^k\rho(q + (1-\rho)b\mathbf{v}\cdot\nabla S). \tag{3.66}$$

What is interesting about this example is while $\mathbb{E}_q = 0$ may be zero, but in no sense is $\mathbb{V}_b\nabla S$ going to be zero. Thus, there is a case for hyperbolic scaling.

3.2.1 Rigorous Hyperbolic Limit

Similar to the parabolic case, we are going to ask if and how the kinetic chemotaxis equation (3.47) converges to (3.64), which will be answered in the result below. Again for this section, we will limit ourselves to the case where $q[\rho](\mathbf{x},\mathbf{v}) = q(\mathbf{v})$, and $b[S](\mathbf{x},\mathbf{v}) := b(\mathbf{x},\mathbf{v})$.

Theorem 4 *Consider the model* (2.1) - (2.3)*, with the assumption* (2.66)*, the initial conditions* $(P_0 = \rho_0 q, S_0 = 0) \in \mathcal{X}$*, and* T *is continuous from this phase space* $\mathcal{X}$ *to* $\mathbb{R}$ *for each* $(\boldsymbol{x},\boldsymbol{v}) \in \mathbb{T}^n \times V$*,*
then as $\epsilon \to 0$*, there is a weak limit*

$$P_\epsilon \rightharpoonup q\rho, \quad S_\epsilon \rightharpoonup S, \tag{3.67}$$

where (P_ϵ, S_ϵ) *satisfy the rescaled kinetic equation*

$$\epsilon(P_\epsilon)_t + \epsilon v \cdot \nabla P_\epsilon = \mu(T_\epsilon[S_\epsilon, \rho_\epsilon]\rho_\epsilon - P_\epsilon), \tag{3.68a}$$

$$(S_\epsilon)_t - D_s \Delta S_\epsilon = \alpha\rho_\epsilon - \frac{1}{\tau} S_\epsilon, \tag{3.68b}$$

$$P_\epsilon(x, v, 0) = P_0(x, v), \quad S_\epsilon(x, 0) = S_0(x), \tag{3.68c}$$

and (ρ, S) *satisfy in the distributional sense*

$$\begin{aligned} &\rho_t + \nabla \cdot (\mathbb{E}_T[S, \rho]\rho) = 0, \\ &S_t - D_s \Delta S = \alpha\rho - \frac{1}{\tau} S, \\ &\rho(x, 0) = \int_V P_0 dv, \quad S(x, 0) = S_0. \end{aligned} \tag{3.69}$$

Proof

Consider (3.68a), integrated over V then

$$(\rho_\epsilon)_t + \nabla \cdot \int_V v P_\epsilon dv = 0, \tag{3.70}$$

again defining $J_\epsilon := \int_V v P_\epsilon dv$. At this point, the main difficulty of the previous proof is not present in this case, since J_ϵ is not explicitly dependent on ϵ; thus, it is clearly uniformly bounded in ϵ along with P_ϵ, and S_ϵ from the *Lemmas* 3, and 5. Again, using (3.68a) to rewrite J_ϵ as

$$J_\epsilon = \int_V \mathbf{v} \left(T_\epsilon[S_\epsilon, \rho_\epsilon]\rho_\epsilon - \frac{\epsilon}{\mu}(P_\epsilon)_t + \mathbf{v} \cdot \nabla P_\epsilon \right) dv. \tag{3.71}$$

Subsituting this back into (3.70) ,

$$(\rho_\epsilon)_t + \nabla \cdot (\mathbb{E}_{T_\epsilon}[S_\epsilon, \rho_\epsilon]\rho_\epsilon) = \frac{\epsilon}{\mu} \nabla (J_\epsilon)_t + \frac{\epsilon}{\mu} \nabla\nabla : \int_V \mathbf{v}\mathbf{v}^T P_\epsilon dv. \tag{3.72}$$

It is clear we need a uniform bound on $\mathbb{E}_{T_\epsilon}$, consider

$$\begin{aligned}\int_{\mathbb{T}^n} |\mathbb{E}_{T_\epsilon}[S_\epsilon, \rho_\epsilon]\rho_\epsilon|^2 dx &= \int_{\mathbb{T}^n} \left| \int_V \mathbf{v} T_\epsilon[S_\epsilon, \rho_\epsilon]\rho_\epsilon dv \right|^2 dx \\ &\leq \int_{\mathbb{T}^n} |\rho_\epsilon|^2 \left| \|\mathbf{v}\|_{L^\infty(V)} \int_V |T_\epsilon[S_\epsilon, \rho_\epsilon]| dv \right|^2 dx \\ &\leq \|\mathbf{v}\|^2_{L^\infty(V)} \|\rho_\epsilon\|^2_{L^2(\mathbb{T}^n)} \\ &\leq \|\mathbf{v}\|^2_{L^\infty(V)} \|\rho_0\|^2_{L^\infty(\mathbb{T}^n)}.\end{aligned} \tag{3.73}$$

This gives us a L^2 bound that is uniform in ϵ allowing us to pass subsequences through $\mathbb{E}_{T_\epsilon}[S_\epsilon, \rho_\epsilon]\rho_\epsilon$. Now we take the inner product with a smooth test function $\phi \in C_c^\infty(\mathbb{T}^n \times [0, T])$

$$\langle (\rho_\epsilon)_t, \phi \rangle + \langle \nabla \cdot (\mathbb{E}_{T_\epsilon}[S_\epsilon, \rho_\epsilon]\rho_\epsilon), \phi \rangle = \frac{\epsilon}{\mu} \langle \nabla \cdot (J_\epsilon)_t, \phi \rangle + \frac{\epsilon}{\mu} \langle \nabla\nabla : \int_V vv^T P_\epsilon dv, \phi \rangle. \tag{3.74}$$

At this point, we move the derivatives onto the test function

$$\langle \rho_\epsilon, \phi_t \rangle + \langle \mathbb{E}_{T_\epsilon}[S_\epsilon, \rho_\epsilon]\rho_\epsilon, \nabla\phi \rangle = \frac{\epsilon}{\mu} \langle J_\epsilon, \nabla\phi_t \rangle + \frac{\epsilon}{\mu} \langle \int_V vv^T P_\epsilon dv, \nabla\nabla^T \phi \rangle. \tag{3.75}$$

Now each of the terms is uniformly bounded in ϵ thanks to *Lemmas* 5, and 3 the above computation (3.73). We can then use weak compactness of reflexive spaces to extract a subsequence of solutions of the transport equation (3.47) such that in the limit converges in a distributional sense to solutions to the hyperbolic system (3.69) .□

From the hyperbolic scaling, we have learned important facts about our system; for instance, the symmetry of q plays a large role in determining if the system is diffusion or advection dominated. If q is even, then $\mathbb{E}_q = 0$ then the hyperbolic system (3.63) only consists of higher-order terms. This even symmetry in q is also common in biological systems at the cellular level. In the cellular environments we are interested in, q plays the extracellular matrix (ECM) role, which is mostly composed of collagen fibres. These fibres impart orienteering cues onto cells, a process known as contact guidance [18, 22]. The fibres act like roads in which movement is promoted along both directions

creating a symmetric distribution in q. An example of a non-symmetric directional cue is environmental factors that play a role in migration, such as the earth's magnetic field, the sun and ocean currents[29]. The other fact is that the size of b plays an important role in determining the proper space scaling. It is not entirely clear whether the case of large b is contained in the assumptions we made showing global existence/uniqueness for the kinetic equations (2.1) - (2.3). The conflicting assumption is (2.66), since we require that the ratio $\frac{q}{b\|\rho_0\|_1}$ is sufficiently small. Now we move onto another hyperbolic system, based on the L^2 Moment closure, where instead of rescaling time and space, we make minimization arguments based on the L^2 norm.

3.3 L^2 Moment Closure

With moment closures, the idea is to directly derive macroscopic equations for statistically meaningful quantities of P, and T like the mean and expectation. These equations are derived by multiplying by $\mathbf{v}$ and integrating over the velocity space V. Although these macroscopic quantities are not technically moments in the probabilistic sense, the form is similar enough to keep the name. Hence, we start by integrating (1.11)

$$\left(\int_V P dv\right)_t + \nabla \cdot \int_V \mathbf{v} P d\mathbf{v} = 0. \tag{3.76}$$

It is important to note this is the mass conservation equation (1.3) from before; however, this time we will denote the macroscopic quantities as

$$m^0 := \int_V P d\mathbf{v}, \quad m^1 := \int_V \mathbf{v} P d\mathbf{v}, \quad m^2 := \int_V \mathbf{v}\mathbf{v}^T P d\mathbf{v} \tag{3.77}$$

and so on. Now the first two moment equations are given by

$$\begin{aligned} &m^0_t + \nabla \cdot m^1 = 0, \\ &m^1_t + \nabla \cdot m^2 = \mu m^0 (E_q[\rho] + (1 - m^0)\mathbb{V}_b[S]\nabla S) - \mu m^1, \end{aligned} \tag{3.78}$$

As we can see, each moment equation will have a higher moment than the evolved quantity. Consequently, we need a way to close the system of equations. There are a couple of ways to do this, which involve an approximation of the highest moment. Examples of these are equilibrium approximation and L^2 minimization. The equilibrium approximation is where the highest moment is taken to be at the equilibrium. By using the L^2 minimization, we obtain a different approximation by projecting $P(\mathbf{x}, \mathbf{v}, t)$ on to the subspace $span\{m^0(\mathbf{x}, t),\, m^1(\mathbf{x}, t)\}$ via minimizing the L^2 norm with the constraint that the first two moments are equal [26]. For this section, we are going to perform the L^2 minimization on the second moment. It is worth noting that this process can be done on higher moments as well [25]. We introduce the following functional $H : L^2(V) \to L^2(V)$, and Lagrangian multipliers $\Lambda^0 \in \mathbb{R}$ and $\Lambda^1 \in \mathbb{R}^n$

$$H[u] := \frac{1}{2}\int_V u^2 dv - \Lambda^0\left(\int_V u dv - m^0\right) - \Lambda^1 \cdot \left(\int_V v u dv - m^1\right). \tag{3.79}$$

Computing the first variation of this functional, we have

$$\frac{\delta}{\delta u} H[u] = u - \Lambda^0 - \Lambda^1 \cdot v.$$

If we look at the second variation, we have $\delta^2 H[u] > 0$ trivially. Thus, there exists a unique minimum. Then setting $\delta H[u] = 0$, we arrive at the following minimum

$$u = \Lambda^0 + \Lambda^1 \cdot v. \tag{3.80}$$

The Lagrangian multipliers are determined by the constraints,

$$m^0 = \int_V u dv = \int_V \Lambda^0 dv + \int_V v \cdot \Lambda^1 dv, \tag{3.81}$$

$$\Lambda^0 = \frac{m^0}{|V|}, \tag{3.82}$$

where $|V|$ is the volume of the velocities

$$|V| = \int_V dv,$$

and

$$m^1 = \int_V vudv = \int_V v(\Lambda^1 \cdot v)dv + \int_V \Lambda^0 vdv, \tag{3.83}$$

$$= \Lambda^1 \int_V vv^T dv = \Lambda^1 \frac{|V|}{3n}(s_2^3 - s_1^3)\mathbb{I}, \tag{3.84}$$

$$\Lambda^1 = \frac{3n}{|V|(s_2^3 - s_1^3)}. \tag{3.85}$$

Thus, for this system, our minimizer takes the form,

$$u_{min}(t, \mathbf{x}, \mathbf{v}) = \frac{1}{|V|}\left(m^0(t, \mathbf{x}) + \gamma(\mathbf{v} \cdot m^1(t, \mathbf{x}))\right), \tag{3.86}$$

where $\gamma := \frac{3n}{s_2^3 - s_1^3}$. With this approximate cell density distribution, we can approximate m^2

$$m^2(u_{min}) = \int_V vv^T u_{min} dv = \frac{1}{|V|}\left(\int_V vv^T m^0 dv + \gamma m^1 \cdot \int_V (vv^T)vdv\right), \tag{3.87}$$

$$= \gamma m^0 \mathbb{I}. \tag{3.88}$$

To end this process, we replace the second moment $m^2(P)$ in (3.78) with $m^2(u_{min})$, allowing us to close (3.78). Note that since $m^2(p) \neq m^2(u_{min}) \implies (m^0(p), m^1(p), S) \neq (m^0(u_{min}), m^1(u_{min}), S)$. For this reason, we introduce capital letters for this new system

$$M_t^0 + \nabla \cdot M^1 = 0, \tag{3.89}$$

$$M_t^1 + \gamma \nabla M^0 = \mu\left(\mathbb{E}_q[M^0] + (1 - M^0)\mathbb{V}_b[S]\mathbf{v} \cdot \nabla S\right) M^0 - \mu M^1, \tag{3.90}$$

$$S_t - D_s \Delta S = \alpha M^0 - \frac{1}{\tau} S. \tag{3.91}$$

There are many useful things to note about this system; the first is that this is the first system that we have derived quasi-linear, a property retained from the kinetic equation. It is also worth remarking that equations (3.89), and (3.90) have the form of the generalized *Cattaneo system* [8, 34]. The Cattaneo model was originally derived from *Cattaneo's law* as a modification to Fourier's law

of heat conduction, where the heat flux $h(\mathbf{x}, t)$ is related to the temperature $w(\mathbf{x}, t)$ by the equation

$$\tau_a h_t + h = -D\nabla w. \tag{3.92}$$

Fourier's law is reobtained by taking the τ_a constant to zero, representing the time that material takes to adapt. Together with the conservation of temperature, we obtain the *Cattaneo system*

$$\begin{aligned} w_t + \nabla \cdot h &= 0, \\ \tau_a h_t + h &= -D\nabla h. \end{aligned} \tag{3.93}$$

This model has a particularly attractive trait that information propagates at a finite speed, which the classical heat equation lacks. There are a few cases of the Cattaneo model being used to describe biological populations, such as Hadeler [24]. Similar to our model, Dolak and Hillen [16] created a chemotaxis model through the kinetic L^2 moment closure method, taking the turning kernel to be

$$T(\mathbf{v}, \mathbf{v}', S, \nabla S) := \frac{\mu}{|V|}\left(1 - \frac{n}{s^2} V(m_0, S)\mathbf{v} \cdot \nabla S\right), \tag{3.94}$$

where $V(u, S)$ is of the density control type, with $V(\bar{u}, S) = 0$ for some $\bar{u} > 0$. The above turning kernel has a lot of the same features to our turning kernel (1.6); for instance, the constant turning rate μ, independence from $\mathbf{v}'$, and density control structure. In fact, if $q(\mathbf{v})$ and $b(\mathbf{v})$ are taken to be uniform distributions, our turning kernel simplifies to the model proposed by Dolak (3.94). The key difference between the models are the quantities $\mathbb{E}_q$ and $\mathbb{V}_b$.

In Dolak and Hillen's paper [16] they apply the Cattaneo model to two biological examples: the slime mold *Dictyotelium discoideum* and the bacterium *Salmonella typhimurium*. For the slime mold, their simulations agree with the results made in the experiments made at the Firtel Lab of the University of California, San Diego [21]. In their experiments, they observed transitions from many small maxima to a few large aggregations. Similarly, Dolak and Hillen's results for the bacterium closely matched the experimental observations of Berg and Budrene (see Woodward et al. [57]).

Let us continue with the general theory. We can consider a further assumption, that the $M_t^1 \sim \mathcal{O}(\epsilon)$, or the first moment changes in time on a slower time scale than the zeroth moment. Then up to first order in ϵ we have

$$\gamma \nabla M^0 = \mu(\mathbb{E}_q + (1 - M^0)\mathbb{V}_b \mathbf{v} \cdot \nabla S)M^0 - \mu M^1.$$

Solving for M^1, we have

$$M^1 = (\mathbb{E}_q + (1 - M^0)\mathbb{V}_b \mathbf{v} \cdot \nabla S)M^0 - \frac{\gamma}{\mu}\nabla M^0.$$

Substituting this expression into the mass conservation equation (3.89),

$$M_t^0 + \nabla(\mathbb{E}_T M^0) = \frac{\gamma}{\mu}\Delta M^0, \tag{3.95}$$

where $\mathbb{E}_T$ is defined in (3.65), now our equation represents a mix between the previous hyperbolic and parabolic cases, the advection term, and isotropic diffusion term.

3.4 Equilibrium Closure

Now we will examine the other moment closure method, the equilibrium closure. For this method, we will close the system by calculating the higher moments using the equilibrium distribution of $P(\mathbf{x}, \mathbf{v}, t)$, instead of minimizing the L^2 norm. The equilibrium closure is a well-established method in [12]. Like the previous moment closure method, we begin by integrating (1.11) over the velocity space V

$$\int_V P_t(\mathbf{v}, \mathbf{x}, t)d\mathbf{v} + \int_V \mathbf{v} \cdot \nabla_{\mathbf{x}} P(\mathbf{v}, \mathbf{x}, t)d\mathbf{v} = 0, \tag{3.96}$$

but this time we will define $P(\mathbf{x}, \mathbf{v}, t) = \hat{P}(\mathbf{x}, \mathbf{v}, t)\rho(\mathbf{x}, t)$ where this new quantity $\hat{P}$ has the property of being a probability distribution. With this definition, we can rewrite the above equation as

$$\rho_t + \nabla_{\mathbf{x}}(\mathbb{E}_{\hat{P}}\rho) = 0. \tag{3.97}$$

Again, this is the same mass conservation equation as in the L^2 moment closure, but this time it is written in terms of the cell density's mean velocity. Like the L^2 moment closure method, we apply the process again by first multiplying (1.11) by $\mathbf{v}$ then integrating over V

$$\int_V \mathbf{v} P_t(\mathbf{v},\mathbf{x},t)d\mathbf{v} + \int_V \mathbf{v}\mathbf{v}^T \nabla_{\mathbf{x}} P(\mathbf{v},\mathbf{x},t)d\mathbf{v} = \int_V \mathbf{v}\mathcal{L}P(\mathbf{v},\mathbf{x},t)d\mathbf{v}. \tag{3.98}$$

We use the following identity to rewrite this equation in terms of the mean, expectation, and variance of P,

$$\begin{aligned}
\mathbb{V}_{\hat{P}} &= \int_V (\mathbf{v}-\mathbb{E}_{\hat{P}})(\mathbf{v}-\mathbb{E}_{\hat{P}})^T \hat{P} d\mathbf{v}, && (3.99)\\
&= \int_V \mathbf{v}\mathbf{v}^T \hat{P} d\mathbf{v} - 2\int_V \mathbf{v}\mathbb{E}_{\hat{P}}^T \hat{P} d\mathbf{v} + \int_V \mathbb{E}_{\hat{P}}\mathbb{E}_{\hat{P}}^T \hat{P} d\mathbf{v}, && (3.100)\\
&= \int_V \mathbf{v}\mathbf{v}^T \hat{P} d\mathbf{v} - \int_V \mathbb{E}_{\hat{P}}\mathbb{E}_{\hat{P}}^T \hat{P} d\mathbf{v}. && (3.101)
\end{aligned}$$

We retrieve an equation in terms of ρ, $E_{\hat{p}}$, and $\mathbb{V}_{\hat{p}}$

$$(\mathbb{E}_{\hat{p}}\rho)_t + \nabla_x(\mathbb{E}_{\hat{p}}\mathbb{E}_{\hat{p}}^T\rho + \mathbb{V}_{\hat{p}}\rho) = \int_V \mathbf{v}\mathcal{L}P(\mathbf{v},\mathbf{x},t)d\mathbf{v}. \tag{3.102}$$

Here is the conservation of population flux equation ($\mathbb{E}_{\hat{P}}\rho$) with an acceleration due to the turning operator. From a fluid dynamics point of view, $\mathbb{V}_{\hat{P}}\rho$ plays the role of the pressure, directing the flow from a volume of high to low pressure or, in this context directing flow from diffusive to directed environments. For our turning operator (1.6), (3.102) becomes

$$(\mathbb{E}_{\hat{P}}\rho)_t + \nabla_x(\mathbb{E}_{\hat{P}}\mathbb{E}_{\hat{P}}^T\rho + \mathbb{V}_{\hat{P}}\rho) = \mu\rho(\mathbb{E}_q[\rho] - \mathbb{E}_{\hat{P}}) + \mu\rho(1-\rho)\mathbb{V}_b[S]\nabla_{\mathbf{x}}S. \tag{3.103}$$

We can repeat the process of multiplying by $\mathbf{v}$ and integrating to get an equation for $\mathbb{V}_{\hat{P}}$, but this will result in a higher moment appearing in the equation. At this point, we need a way to close the system. We close the system by approximating the highest moment, $\mathbb{V}_{\hat{P}}$ at the equilibrium distribution P_e.

Formally this occurs when

$$\mathcal{L}P_e(\mathbf{v},\mathbf{x},t)=0,$$

which takes the form

$$P_e=\rho(q[\rho]+(1-\rho)b[S]\mathbf{v}\cdot\nabla_x S). \tag{3.104}$$

Then the expectation of the equilibrium distribution is

$$\begin{aligned}\mathbb{E}_{\hat{P}_e}\rho&=\int_V \mathbf{v}\hat{P}_e\rho\mathbf{v}=\int_V \mathbf{v}\rho(q[\rho]+(1-\rho)b[S]\mathbf{v}\cdot\nabla_x S)d\mathbf{v},\\&=(\mathbb{E}_q[\rho]+(1-\rho)\mathbb{V}_b[S]\nabla_{\mathbf{x}}S)\rho.\end{aligned} \tag{3.105}$$

Finally, we can compute the equilibrium variance as

$$\mathbb{V}_{\hat{P}_e}\rho=\int_V(\mathbf{v}-\mathbb{E}_q-(1-\rho)\mathbb{V}_b\nabla_{\mathbf{x}}S)(\mathbf{v}-\mathbb{E}_q-(1-\rho)\mathbb{V}_b\nabla_{\mathbf{x}}S)^T\rho(q+(1-\rho)b\mathbf{v}\cdot\nabla_x S)d\mathbf{v}. \tag{3.106}$$

Using the bilinearity of the outer product, and the various properties of the turning kernel, we can simplify the above expression into terms of variance, and expectation of $q[\rho]$, and $b[S,\rho]$

$$\begin{aligned}(\mathbb{V}_{\hat{P}_e})_{ij}\rho=&(\mathbb{V}_q[\rho])_{ij}\rho-(\nabla S)_l\Big((E_q[\rho])_j(\mathbb{V}_b[S])_{il}+(E_q[\rho])_i(\mathbb{V}_b[S])_{jl}\Big)\rho(1-\rho)\\&-(\nabla S)_l(\nabla S)_k(\mathbb{V}_b[S])_{kj}(\mathbb{V}_b[S])_{il}\rho(1-\rho)^2.\end{aligned} \tag{3.107}$$

Now, approximating $\mathbb{V}_{\hat{P}}\approx\mathbb{V}_{\hat{P}_e}$ in (3.103), yields the following equation,

$$\begin{aligned}&(\mathbb{E}_{\hat{P}}\rho)_t+\nabla(\mathbb{E}_{\hat{P}}\mathbb{E}^T_{\hat{P}}\rho+\mathbb{V}_q\rho)-\mu\rho(\mathbb{E}_q-\mathbb{E}_{\hat{P}})=\mu\rho(1-\rho)\mathbb{V}_b\nabla S\\&+\nabla\bigg(\rho(1-\rho)\Big(\mathbb{V}_b\nabla S\mathbb{E}_q^T+\mathbb{E}_q(\mathbb{V}_b\nabla S)^T+(1-\rho)\mathbb{V}_b(\nabla S)(\nabla S)^T\mathbb{V}_b^T\Big)\bigg).\end{aligned} \tag{3.108}$$

In this form, the effects of the two environmental cues on the population flux are distinct. The left-hand side is entirely due to the fibre distribution

of q, whereas the right-hand side consists of the chemoattractant's influence. The first term on the right is the one that we have seen throughout the other approximation methods. The term relaxes the population flux to the chemoattractant concentration. The new term is the broad gradient term representing the interaction between the fibre distributions, the chemoattract (q and b), and the chemotaxis's interaction with itself. These terms will influence the population to flow in directions were b and q align.

Remark 5 *By assuming the environment is isotropic for both b and q, and that the interaction terms are small* (3.108) *reduces to the system proposed by Filbet [20].*

$$\mathbb{E}_q[\rho] = \mathbb{E}_{\hat{P}}, \qquad \mathbb{V}_q[\rho] = \theta(\rho)\mathbb{I}, \tag{3.109}$$

$$\mathbb{V}_b[S,\rho] = \frac{1}{\mu}\mathbb{I}, \tag{3.110}$$

where $\theta(\rho)$ is an increasing scalar function. These assumptions yield,

$$\begin{aligned}(\mathbb{E}_{\hat{P}}\rho)_t + \nabla(\mathbb{E}_{\hat{P}}\mathbb{E}_{\hat{P}}^T\rho + \rho\theta(\rho)) &= \rho\nabla S \\ &+ \frac{1}{\mu}\nabla\bigg(\rho\Big(\nabla S\mathbb{E}_{\hat{P}}^T + \mathbb{E}_{\hat{P}}\nabla S^T + \frac{1}{\mu}(\nabla S)(\nabla S)^T\Big)\bigg).\end{aligned} \tag{3.111}$$

Now, assuming that $1/\mu << 1$, the interaction terms disappear.

We can further simplify the system (3.108), by consider the case where the flux ($\mathbb{E}_{\hat{p}}\rho$) quickly relaxes to its equilibrium. This assumption is done by setting the material derivative of the flux to be zero $\mathcal{D}_t\mathbb{E}_{\hat{p}}\rho := (\mathbb{E}_{\hat{p}}\rho)_t + \nabla(\mathbb{E}_{\hat{p}}\mathbb{E}_{\hat{p}}^T\rho)$ in (3.108)

$$\begin{aligned}&\nabla(\mathbb{V}_q\rho) = \mu\rho(\mathbb{E}_q - \mathbb{E}_{\hat{P}}) + \mu\rho(1-\rho)\mathbb{V}_b\nabla S \\ &+ \nabla\bigg(\rho(1-\rho)\Big(\mathbb{V}_b\nabla S\mathbb{E}_q^T + \mathbb{E}_q(\mathbb{V}_b\nabla S)^T + (1-\rho)\mathbb{V}_b(\nabla S)(\nabla S)^T\mathbb{V}_b^T\Big)\bigg).\end{aligned}$$

Solving for $\mathbb{E}_{\hat{P}}\rho$, and substituting into the mass conservation law equation

(3.97) leads to

$$\rho_t + \nabla(\mathbb{E}_T\rho) - \frac{1}{\mu}\nabla\nabla : (\mathbb{V}_q\rho)$$
$$= \frac{1}{\mu}\nabla\nabla : \left(\rho(1-\rho)\Big(\mathbb{V}_b\nabla S\mathbb{E}_q^T + \mathbb{E}_q(\mathbb{V}_b\nabla S)^T + (1-\rho)\mathbb{V}_b(\nabla S)(\nabla S)^T\mathbb{V}_b^T\Big)\right). \tag{3.112}$$

The above equation is similar to the L^2 moment closure in the slow momentum change case, with the same advection terms and a similar diffusion term. The main difference between the two-moment closures is the presence of anisotropic diffusion and the interaction terms.

3.5 Conclusion

Now that we have gone through the various scaling methods and moment closure techniques, we will summarize and contrast our findings. We will look at the form of the limiting equations and show relations between them. We will reexamine the underlying assumptions of the approximation methods. For this section we will ignore the chemoattractant equation, and for convenience of comparison, we will unify the notation $\rho = M_0$, $\mathbf{x} = \xi$, and $t = \tau$

3.5.1 Limit equations

The four approximation methods lead to these six equations:

- Parabolic Scaling (3.16),

$$\rho_t - \frac{1}{\mu}\nabla\left(\nabla\left(\mathbb{V}_q\rho + \mathbb{E}_q\mathbb{E}_q^T\rho\right) - \rho(1-\rho)\mathbb{V}_b\nabla S\right) = 0; \tag{PS}$$

- Hyperbolic Scaling (3.53),

$$\rho_t + \nabla\cdot(\mathbb{E}_q\rho) = 0; \tag{HS}$$

- Hyperbolic scaling with first order correction (3.63),

$$\rho_t + \nabla \cdot (\mathbb{E}_q \rho) - \left(\frac{\epsilon}{\mu}\right)\left[\nabla\nabla : \left((\mathbb{V}_q + \mathbb{E}_q \mathbb{E}_q^T)\rho\right) - \nabla(((\mathbb{E}_q)_\rho \rho + \mathbb{E}_q)\nabla(\mathbb{E}_q \rho))\right] + \epsilon \nabla\nabla S : (\rho(1-\rho)\mathbb{V}_b) = 0; \tag{HC}$$

- Hyperbolic Scaling for large b (3.69),

$$\rho_t + \nabla \cdot (\mathbb{E}_T \rho) = 0; \tag{HSb}$$

- L^2 Moment Closure (3.89),

$$\rho_t + \nabla(E_T \rho) = \frac{\gamma}{\mu}\Delta\rho; \tag{L2}$$

- Equilibrium Closure (3.112),

$$\rho_t + \nabla(\mathbb{E}_T \rho) - \frac{1}{\mu}\nabla\nabla : (\mathbb{V}_q \rho) = \frac{1}{\mu}\nabla\nabla : \left(\rho(1-\rho)\Big(\mathbb{V}_b \nabla S \mathbb{E}_q^T + \mathbb{E}_q(\mathbb{V}_b \nabla S)^T + (1-\rho)\mathbb{V}_b(\nabla S)(\nabla S)^T \mathbb{V}_b^T\Big)\right). \tag{EC}$$

With all the equations laid out, we can see that the scalings and moment closures lead to quite different equations. However, there is overlap between the various approximations. We summarize these overlaps in the following *Lemma*. It is clear that (EC) only overlaps with the other equations if the interaction terms are small. For the sake of the following *Lemma*, we will assume $\mathbb{V}_b = \mathcal{O}(\epsilon)$ with $\mu = \mathcal{O}(\epsilon^{-1})$, for (EC).

Lemma 6

1. ***(Diffusion-dominated)*** *In the case* $\mathbb{E}_q = 0$, *or* $\mathbb{E}_q = \mathcal{O}(\epsilon^2)$ *the approximations* (PS),(HC),(EC) *lead to the parabolic limit* (PS), *while* (HS) *is trivial.*

2. ***(Drift-diffusion)*** *If* $\mathbb{E}_q = \mathcal{O}(\epsilon)$*, then* (HC) *and* (EC) *coincide to leading order.*

3. ***(Drift-dominated)*** *if* $\mathbb{E}_q = \mathcal{O}(\epsilon)$*, and* $\mathbb{V}_q = \mathcal{O}(\epsilon)$ *(or* $\mu = \mathcal{O}(\epsilon^{-1})$*), then* (HC) *and* (HSb) *coincide to leading order.*

4. ***(Isotropic)*** *if* $q(\boldsymbol{v})$ *is the uniform distribution, then* (L2)*, and* (EC) *coincide to leading order.*

Moving onto the approximation methods' underlying assumptions, there are two main types of the scalings, which consist of the parabolic and hyperbolic scalings and two moment closures consisting of the L^2 moment closure and Equilibrium closure. The fact that the above scalings, closure methods lead to very different equations is a bit disturbing. It seems to leave the researcher hanging in the air, unable to choose the best method. However, when looking at the biological situations relevant to the various methods, a distinction becomes clear. Here, we summarize the underlying biological assumptions.

- **(Parabolic)** Corresponds to a time scale where particles are fast and turn frequently, with movement close to a Brownian random movement [29]. An example of the time scale is the example we used to motivate rescaling, the bacteria *E.coli*, which has a turning rate of around $\mu \approx 1/sec$, and average speed of $|\mathbf{v}| \approx 10^{-2} mm/sec$. In most parabolic scalings, there is no clear directional cue, other than the directional bias as a result of anisotropy of the variance, covariance matrix $\mathbb{V}_q$, and $\mathbb{E}_q \mathbb{E}_q^T$, but the addition of the chemotactic terms creates a directional cue.

- **(Hyperbolic)** Again, the time-space scale is where particles are fast and turn frequently, but this time there is a clear directional cue provided by the unperturbed environment q. An example is the migration of sea turtles, where their movement is directed mainly by the Earth's magnetic field [41].

- **(L^2 moment closure)** This approximation can be seen as minimizing the L^2 norm. An effect of this choice is that we are smoothing out the

oscillations, consider altering the functional for $a \in \mathbb{R}$ (3.79)

$$H_a[u] := \frac{1}{2}\int_V (u-a)^2 dv - \Lambda^0\left(\int_V u dv - m^0\right) - \Lambda^1 \cdot \left(\int_V v u dv - m^1\right), \tag{3.113}$$

note that this change does not affect the resulting minimizer. Thus, in a sense, we are minimizing $\|u-a\|_2$, which is a measure of oscillations around a. The qualitative effect is that the approximate solution is smoother than the true solution [26].

- **(Equilibrium Closure)** For this approximation, we are essentially saying that the second moment is close to the equilibrium distribution, and we take the population flux to relax to the equilibrium rapidly.

After going through the underlying assumptions, the split between the scaling and closure methods becomes more apparent. The scaling methods require intimate knowledge of the turning rate and average speed of the objects involved and an understanding of the scale of macroscopic dynamics. For these reasons, the scaling methods are prevalent for cellular processes, since there is a substantial amount of statistics for speed and turning rates, and the lab-scale makes a natural macroscopic scale. The strength of $\mathbb{E}_q$ plays the most significant role in the symmetry breaking between the parabolic scaling and hyperbolic scaling. If $\mathbb{E}_q$ is large compared to the variance $\mathbb{V}_q$, we are in the advection dominated regime; therefore, the hyperbolic scaling (HC) is the proper choice. If $\mathbb{E}_q$ is very small, we have entered the diffusive regime, and the parabolic scaling (PS) is the appropriate choice. From the structure of the equations derived by moment closures (L2) and (EC), we can see that they play the role of the middle man between the hyperbolic and parabolic scaling by having both advection and diffusion effects.

Unlike the scaling methods, the closure methods do not have clear indicators like the magnitude of parameters, but rather are based on the higher-order moments' structure. Both methods assume that the first moment relaxes quickly to the equilibrium, but the difference is how they treat the second moment. For the L^2 closure, the assumption is that the second moment's oscillations are small. The result is a system where there is no anisotropic diffusion.

The assumption is that the second moment is close to the second moment of the equilibrium for the equilibrium closure. The closure methods are useful when knowledge of individual velocities are unknown or highly variable, and there is evidence that the second moment is either free of oscillations or close to its equilibrium.

Chapter 4

Numerics

In this chapter, we will numerically explore the effect of anisotropy on chemotaxis. For this exploration, we will return to the example of the endothelial cells randomly distributed to form a vascular network. We will describe this motion using the parabolic limit (3.33). For the domain, we will consider the two-dimensional square $[0, L] \times [0, L]$ with a periodic boundary condition. We discretize this square into smaller squares with side lengths of h, and index these squares by the indices j, k, representing the x-axis and y-axis. Both indices run from $[1, N]$, where $N = \frac{L}{h}$.

4.1 Hybrid FVFD Scheme

For the numerical scheme, we will closely follow the method proposed by Chertock in [13]. Chertock derived a second-order hybrid Finite volume finite element scheme for the classical Keller Segel model

$$\rho_t = \nabla(\nabla\rho - \rho\nabla S), \tag{4.1}$$

$$S_t = \Delta S + \rho - S. \tag{4.2}$$

They were able to show positivity preservation for this scheme based on reasonable CFL conditions, making it ideal for our problem. Since our system has added complexities, namely the anisotropic terms, we had to alter the scheme for our model. For this reason, we will go through the scheme in detail to

exhibit these differences. Although it is unclear if our system holds the same positivity result as in [13], our numerical results are strictly positive. To begin, we have to write (3.33) in the form of fluxes along the axis; for this purpose, we write (3.33) in two dimensions

$$\frac{d\rho}{dt} - \left(\frac{1}{\mu}\left(\mathbb{V}_q^{1,1}\rho\right)_x + \frac{1}{\mu}\left(\mathbb{V}_q^{1,2}\rho\right)_y - \rho(1-\rho)\left(\mathbb{V}_b^{1,1}S_x + \mathbb{V}_b^{1,2}S_y\right)\right)_x \tag{4.3}$$

$$- \left(\frac{1}{\mu}\left(\mathbb{V}_q^{2,1}\rho\right)_x + \frac{1}{\mu}\left(\mathbb{V}_q^{2,2}\rho\right)_y - \rho(1-\rho)\left(\mathbb{V}_b^{2,1}S_x + \mathbb{V}_b^{2,2}S_y\right)\right)_y = 0, \tag{4.4}$$

$$S_t = \Delta S + \alpha\rho - \frac{1}{\tau}S. \tag{4.5}$$

On the above mesh, the goal is to write the system as a semi-discrete hybrid FVFD scheme, which takes the form of

$$\frac{d\bar{\rho}_{j,k}}{dt} = -\frac{\mathcal{F}_{j+\frac{1}{2},k} - \mathcal{F}_{j-\frac{1}{2},k} + \mathcal{F}_{j,k+\frac{1}{2}} - \mathcal{F}_{j,k+\frac{1}{2}}}{h}, \tag{4.6}$$

$$\frac{dS_{j,k}}{dt} = \Delta_{j,k}S + \alpha\rho_{j,k} - \frac{1}{\tau}S_{j,k}. \tag{4.7}$$

Where the averaged cell density is $\bar{\rho}_{j,k} \approx \frac{1}{h^2}\int_{I_{j,k}} \rho(x,y,t)dxdy$, $S_{j,k}$, and $\rho_{j,k}$ are the point values of the chemoattractant and cell density respectively. $\mathcal{F}_{j,k}$ are the numerical fluxes in the x and y directions, and $\Delta_{j,k}$ is the discrete Laplacian. We can write the numerical fluxes as follows

$$\mathcal{F}_{j+\frac{1}{2},k} = \bar{\rho}_{j+\frac{1}{2},k}(1-\bar{\rho}_{j+\frac{1}{2},k})u_{j+\frac{1}{2},k} - \frac{1}{\mu}\left(\left(\mathbb{V}_q^{1,1}\rho\right)_x\right)_{j+\frac{1}{2},k} - \frac{1}{\mu}\left(\left(\mathbb{V}_q^{1,2}\rho\right)_y\right)_{j+\frac{1}{2},k}, \tag{4.8}$$

$$\mathcal{F}_{j,k+\frac{1}{2}} = \bar{\rho}_{j,k+\frac{1}{2}}(1-\bar{\rho}_{j,k+\frac{1}{2}})v_{j,k+\frac{1}{2}} - \frac{1}{\mu}\left(\left(\mathbb{V}_q^{2,1}\rho\right)_x\right)_{j,k+\frac{1}{2}} - \frac{1}{\mu}\left(\left(\mathbb{V}_q^{2,2}\rho\right)_y\right)_{j,k+\frac{1}{2}}, \tag{4.9}$$

where u, and v chemotactic velocity,

$$u_{j+\frac{1}{2},k} = (\mathbb{V}_b^{1,1})_{j+\frac{1}{2},k}(S_x)_{j+\frac{1}{2},k} + (\mathbb{V}_b^{1,2})_{j+\frac{1}{2},k}(S_y)_{j+\frac{1}{2},k}, \tag{4.10}$$

$$v_{j,k+\frac{1}{2}} = (\mathbb{V}_b^{2,1})_{j,k+\frac{1}{2}}(S_x)_{j,k+\frac{1}{2}} + (\mathbb{V}_b^{2,2})_{j,k+\frac{1}{2}}(S_y)_{j,k+\frac{1}{2}}. \tag{4.11}$$

Now, the scaled cell density derivatives are computed via central differences

$$\begin{aligned}
\left(\left(\mathbb{V}_q^{1,1}\rho\right)_x\right)_{j+\frac{1}{2},k} &= \frac{\left(\mathbb{V}_q^{1,1}\right)_{j+1,k}\bar{\rho}_{j+1,k} - \left(\mathbb{V}_q^{1,1}\right)_{j,k}\bar{\rho}_{j,k}}{h},\\
\left(\left(\mathbb{V}_q^{1,2}\rho\right)_y\right)_{j+\frac{1}{2},k} &= \frac{\left(\mathbb{V}_q^{1,2}\right)_{j+\frac{1}{2},k+1}\rho_{j+\frac{1}{2},k+1} - \left(\mathbb{V}_q^{1,2}\right)_{j+\frac{1}{2},k-1}\rho_{j+\frac{1}{2},k-1}}{2h},\\
\left(\left(\mathbb{V}_q^{2,1}\rho\right)_x\right)_{j,k+\frac{1}{2}} &= \frac{\left(\mathbb{V}_q^{2,1}\right)_{j+1,k+\frac{1}{2}}\rho_{j+1,k+\frac{1}{2}} - \left(\mathbb{V}_q^{2,1}\right)_{j-1,k+\frac{1}{2}}\rho_{j-1,k+\frac{1}{2}}}{2h},\\
\left(\left(\mathbb{V}_q^{2,2}\rho\right)_x\right)_{j,k+\frac{1}{2}} &= \frac{\left(\mathbb{V}_q^{2,2}\right)_{j,k+1}\bar{\rho}_{j,k+1} - \left(\mathbb{V}_q^{2,2}\right)_{j,k}\bar{\rho}_{j,k}}{h}.
\end{aligned}$$

The Chemotactic derivatives $(S_x)_{j+\frac{1}{2},k}$, $(S_y)_{j+\frac{1}{2},k}$,$(S_x)_{j,k+\frac{1}{2}}$, and $(S_y)_{j,k+\frac{1}{2}}$ are computed similarly. The point values $\rho_{j+\frac{1}{2},k}$, and $\rho_{j,k+\frac{1}{2}}$ are computed in a upwind manner

$$\rho_{j+\frac{1}{2},k} = \begin{cases} \rho^E_{j,k}, & \text{if } u_{j+\frac{1}{2},k} > 0,\\ \rho^W_{j+1,k}, & \text{otherwise.}\end{cases} \qquad \rho_{j,k+\frac{1}{2}} = \begin{cases} \rho^N_{j,k}, & \text{if } v_{j,k+\frac{1}{2}} > 0,\\ \rho^S_{j,k+1}, & \text{otherwise.}\end{cases}$$

The one sided point values at the interfaces $\rho^E_{j,k}$, $\rho^W_{j+1,k}$, $\rho^N_{j,k}$, and $\rho^S_{j,k+1}$, are computed using the second order piecewise linear reconstruction

$$\begin{aligned}
\rho^E_{j,k} &= \bar{\rho}_{j,k} + \frac{h}{2}(\rho_x)_{j,k},\\
\rho^W_{j+1,k} &= \bar{\rho}_{j+1,k} - \frac{h}{2}(\rho_x)_{j+1,k},\\
\rho^N_{j,k} &= \bar{\rho}_{j,k} + \frac{h}{2}(\rho_y)_{j,k},\\
\rho^W_{j,k+1} &= \bar{\rho}_{j,k+1} - \frac{h}{2}(\rho_y)_{j,k+1}.
\end{aligned}$$

To ensure that the above point values are second-order and non-negative, slopes are computed adaptively

$$(\rho_x)_{j,k} = \begin{cases} \frac{\bar{\rho}_{j+1,k}-\bar{\rho}_{j-1,k}}{2h}, & \text{if } \bar{\rho}_{j,k} + \frac{\bar{\rho}_{j+1,k}-\bar{\rho}_{j-1,k}}{4} \geq 0,\\ \text{minmod}\left(2\frac{\bar{\rho}_{j+1,k}-\bar{\rho}_{j,k}}{h}, \frac{\bar{\rho}_{j+1,k}-\bar{\rho}_{j-1,k}}{2h}, 2\frac{\bar{\rho}_{j,k}-\bar{\rho}_{j-1,k}}{h}\right), & \text{otherwise,}\end{cases}$$

where the flux limiter minmod

$$\text{minmod}(x_1, x_2, \dots) := \begin{cases} \min(x_1, x_2, \dots), & \text{if } x_i > 0, \forall i, \\ \max(x_1, x_2, \dots), & \text{if } x_i < 0, \forall i, \\ 0, & \text{otherwise.} \end{cases}$$

The positivity of the reconstructed cell density point values is guaranteed by the positivity preserving generalized minmod limiter,[53, 36, **?**, 50] with the assumption that the underlying cell averages are positive. For the discrete Laplacian, we use the standard five-point stencil [23] to obtain a second-order approximation

$$\Delta_{j,k} S = \frac{S_{j+1,k} + S_{j-1,k} - 4S_{j,k} + S_{j,k-1} + S_{j,k+1}}{h^2}.$$

Thus we have derived a second-order semi-discrete method for (3.33)

$$\frac{d\bar{\rho}_{j,k}}{dt} = -\frac{\mathcal{F}_{j+\frac{1}{2},k} - \mathcal{F}_{j-\frac{1}{2},k} + \mathcal{F}_{j,k+\frac{1}{2}} - \mathcal{F}_{j,k+\frac{1}{2}}}{h}, \tag{4.12}$$

$$\frac{dS_{j,k}}{dt} = \Delta_{j,k} S + \alpha \rho_{j,k} - \frac{1}{\tau} S_{j,k}. \tag{4.13}$$

To evolve this semi discrete scheme through time we chose to use a second order adaptive Runge-Kutta scheme [17].

4.2 Parameters

The system has a couple of parameters we have to determine namely, α the production rate of the chemoattractant, τ degradation time, μ the turning rate, D_s diffusion rate of the chemoattractant, finally the forms of the distributions $\rho(\mathbf{x}, t)$, $q(\mathbf{x}, \mathbf{v})$, and $b(\mathbf{x}, \mathbf{v})$. With the purpose of looking at vascular assembly, we can find the constant parameters, $\tau = 3600s$, $\alpha = 1$ from [47], $D_s = 10^{-7} cm/s^2$ from [45], and $\mu = 1785.71/s$ from [48]. We take the initial

condition to be a linear combination of Gaussian's

$$\rho_0(x,y) = \frac{1}{4\pi^2}\sum_{k=1}^{W} e^{\frac{(x-x_l)^2+(y-y_l)^2}{2\sigma^2}}, \tag{4.14}$$

where $\{(x_l, y_l\}_{l=1}^{W}$ is a sequence of random numbers drawn from the uniform distribution on $[0, N]^2$. This initial condition represents a random distribution of cells on a petri dish, which have a radius of σ. From available data of molecular radii [54, 37], we can estimate the radius of a cell to be $\sigma = 0.003\ cm$. With the general parameters defined, we can move onto experiments.

4.3 Vascular Network Formation

In this experiment, we are just interested in replicating previous models' results in looking at vascular network formation as in [47, 20]. In their experiments, they took the randomly distributed cells, with b being uniformly distributed. For the distribution q, the choice is a little more complicated. In [47, 20], they propose a pressure term $P(\rho) = \rho^3$ to deal with cell compression. They derived their models through the moment closure (although they do not assume that the flux relaxes quickly to the equilibrium) taking the form

$$\rho_t + \nabla(\mathbb{E}_{\hat{p}}\rho) = 0, \tag{4.15}$$

$$(\mathbb{E}_{\hat{p}}\rho)_t + \nabla\left(\mathbb{E}_{\hat{p}}\mathbb{E}_{\hat{p}}^T\rho + \rho^3\mathbb{I}\right) = \rho\nabla S, \tag{4.16}$$

however, we can match the pressure term to our anisotropic diffusion tensor $\mathbb{V}_q = \rho^3$, by looking at our moment closure model. One of the critical findings these papers was that the formation of networks for these parameter values bifurcates on the cell density per cm^2 (number of Gaussians per unit area). Their rough estimate was for the critical cell density was 100 $cells/mm^2$

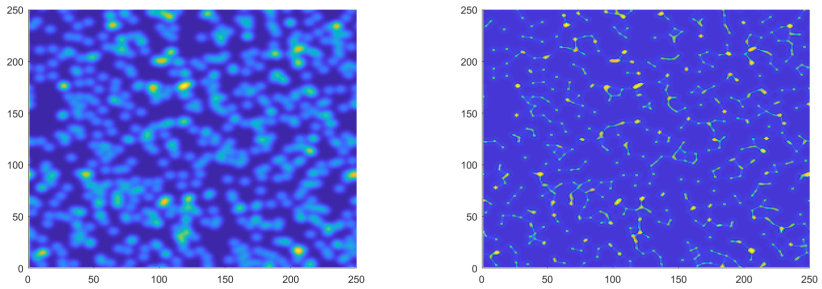

(a) **(b)**

Figure 4.1: Formation of Network: a) Initial condition with cell density of 100 $cells/mm^2$, b) Solution at $1.5s$

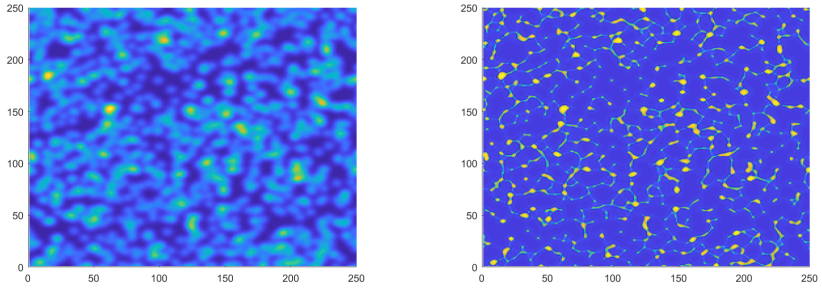

(a) **(b)**

Figure 4.2: Formation of Network: a) Initial condition with cell density of 200 $cells/mm^2$, b) Solution at $1.5s$

In all cases, in figures 4.1, 4.2, and 4.3, structures are forming, but only after hitting a density 200 $cells/mm^2$ is there larger-scale structures like cells forming connected rings. Interestingly, we were able to obtain qualitatively similar results to [47, 20], despite using a different class of equations. This result could be explained by the fact that we are looking at the system's long time behaviour with no clear directional cue provided by q. For our model, this situation is precisely where the parabolic scaling coincides with equilibrium closure (no interaction terms). Although [47, 20] do not take the fast-flux relaxation, it seems that the flux does relax to its equilibrium, evidenced by the similarity between our solutions.

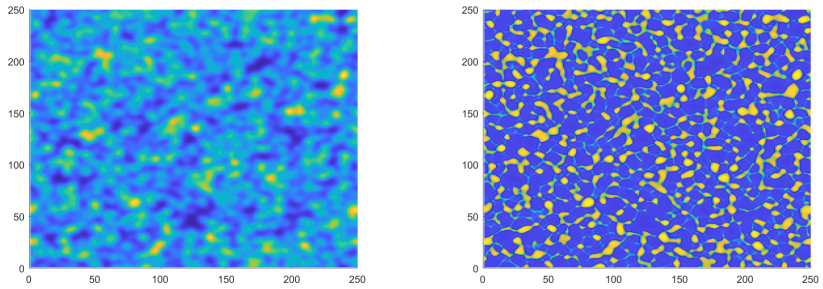

(a) **(b)**

Figure 4.3: Formation of Network: a) Initial condition with cell density of 400 $cells/mm^2$, b) Solution at $1.5s$

4.4 Anisotropic Diffusion

For this experiment, we are interested in looking at the effects of anisotropic diffusion. We take

$$q(\mathbf{v}) = \frac{1}{4\pi I_0(k)} \left(e^{k\mathbf{v}\cdot\mathbf{u}} + e^{-k\mathbf{v}\cdot\mathbf{u}} \right), \quad b = \frac{1}{50}. \tag{4.17}$$

Which means that the variances matrices take the form

$$\mathbb{V}_q = \frac{1}{2}\left(1 - \frac{I_2(k)}{I_0(k)}\right)\mathbb{I} + \frac{I_2(k)}{I_0(k)}\mathbf{u}\mathbf{u}^T, \quad \mathbb{V}_b = \frac{1}{50}\mathbb{I}. \tag{4.18}$$

Taking the fibre direction $\mathbf{u}$ to be along the main diagonal, i.e. $\mathbf{u} = (\frac{1}{\sqrt{2}}, \frac{1}{\sqrt{2}})$.

From the figures 4.4, and 4.5, we can see that having a fibre $\mathbf{u} = (\frac{1}{\sqrt{2}}, \frac{1}{\sqrt{2}})$, severely changes how the system diffuses. Instead of a radial symmetric spread, there is smearing along the main diagonal, and as we increase the concentration parameter, there is a tighter and tighter spread along the diagonal. We can also localize anisotropic effects to regions by taking the concentration parameter to be a function of $\mathbf{x}$, namely

$$k(\mathbf{x}) = 10e^{-\frac{(\mathbf{x}-L/2)^2}{(8\sigma)^2}}, \tag{4.19}$$

Changing the concentration parameter k to depend on $\mathbf{x}$ causes regions

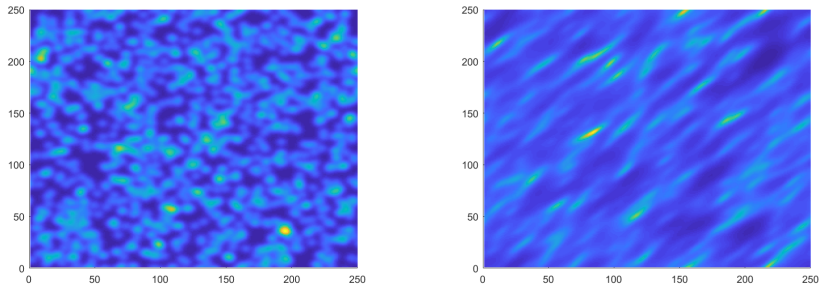

(a) **(b)**

Figure 4.4: Concentration parameter of $k = 5$: a) Initial condition with cell density of 200 $cells/mm^2$, b) Final State at $0.32s$

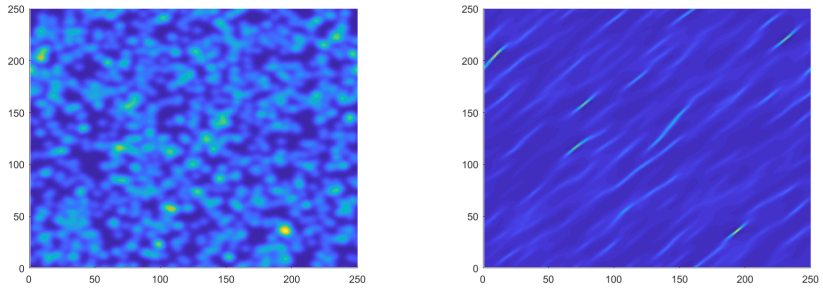

(a) **(b)**

Figure 4.5: Concentration parameter of $k = 10$: a) Initial condition with cell density of 200 $cells/mm^2$, b) Final State at $0.32s$

where nonuniform diffusion reigns, the cross in the center, and the corners where the diffusion is nearly uniform.

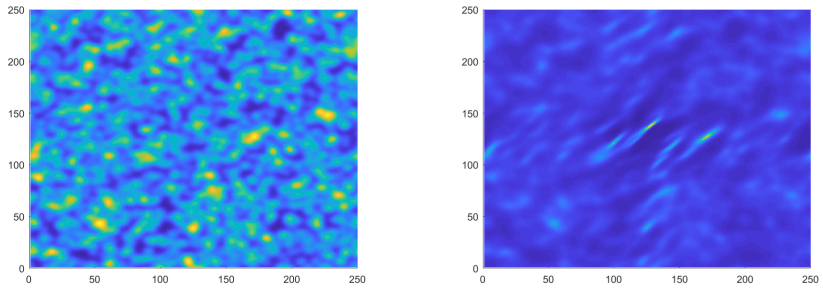

(a) **(b)**

Figure 4.6: Concentration parameter of $k = k(\mathbf{x})$: a) Initial condition with cell density of 200 $cells/mm^2$, b) Solution at $0.32s$

4.5 Chemotactic Mixing

In this experiment, we are going to explore mixing the chemotactic velocities, for this reason, consider

$$\mathbb{V}_b(\mathbf{x}) = \frac{1}{50}\mathbb{I} + \frac{s}{2}\left(A + A^T\right), \tag{4.20}$$

where A is the matrix, and s is the max velocity

$$A = \begin{pmatrix} 0 & \frac{1}{2} \\ \frac{1}{2} & 0 \end{pmatrix}, \quad s = 1/5\ cm/s.$$

Simulating this set of parameters

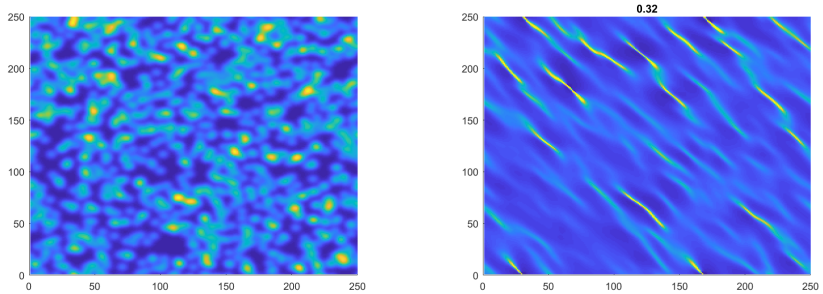

(a) **(b)**

Figure 4.7: Velocity mixing a) Initial condition with cell density of 200 $cells/mm^2$, b) Solution at $0.32s$

From this figure 4.7, we can see that the effect of the chemotaxis mixing is comparable to the effect of non-uniform diffusion as we have seen in the previous experiment. The difference is that the chemotactic mixing seems to affect the diffusion along the diagonal $(-1, 1)$, but the chemotaxis term usually acts as a deterrent, reducing movement away from high-density regions. Therefore, we hypothesize that the chemotaxis term is not promoting movement along the $(-1, 1)$ direction, but discouraging diffusion along $(1, 1)$, while leaving diffusion along $(-1, 1)$ unimpeded giving the structures in the figure 4.7.

4.6 Anisotropic Diffusion vs. Chemotactic mixing

Now we wish to examine the interaction between the fibre distributions q and the chemotactic velocity mixing. For this we consider the q in (4.17), and b in (4.20). According to the previous experiments, these choices of distributions should act in opposition to each other, q along $(1, 1)$, and b along $(-1, 1)$. We take the same initial condition as in previous experiments.

From this time series of figures 4.8, we can see that there seem to be two

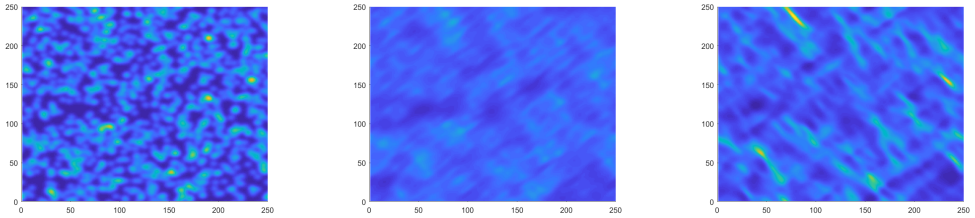

(a) **(b)** **(c)**

Figure 4.8: Anisotropic Diffusion and Velocity Mixing: a) Initial condition with cell density of 200 $cells/mm^2$, b) Solution at 0.0989 s c) Solution at 0.32 s

regimes. The first regime is where the anisotropic diffusion dominates, and we see the smearing of the cells along the positive diagonal. The second regime occurs at the end of the simulation, where the higher density regions are pulled towards the $(-1, 1)$ diagonal, and the lower density regions continue on their

path. The split in dominance occurs because the chemotaxis terms' strength is entirely dependent on the density and time. Since the chemoattractant concentration starts at zero, the anisotropic diffusion initially takes control. This state of affairs continues until the anisotropic diffusion squeezes the solution enough to reach a cell density critical point. From this point on, the chemotaxis terms dominate, inducing movement along the orthogonal diagonal, but only in the high-density regions. The result is this crisscrossing knitting pattern.

We see numerically fascinating patterns. The effects of anisotropy and chemotaxis interact in complicated ways. More research is needed to investigate these observed numerical patterns.

Chapter 5

Conclusion

The principle goal of this thesis is to examine the various approximations of the kinetic chemotaxis equations. In Chapter 1, we derived the kinetic chemotaxis system based on some simple assumptions on how endothelial cells move. First, we assume that a velocity jump process can model a cell's movement, and secondly, that its velocity is influenced by a chemoattractant. In addition, a diffusion equation governs the chemoattractant, and cells cannot arbitrarily compress. We can move from this stochastic model to the kinetic equation via averaging procedures.

From here, we reach the topic of Chapter 2, where we asked the time tested mathematical question of whether the derived set of equations have a solution, and what requirements on the parameters give global solutions. We established local existence/uniqueness using semigroup theory. The whole proof is based on the idea that a positive turning kernel implies that the solution is positive. We cannot guarantee that the turning kernel remains positive, due to the functional dependence on ρ and ∇S. However, we do know that the turning kernel remains positive for some closed set. Building off of this fact, we can use a translational symmetry to bound ρ. The bounds in ρ allow us to construct classical solutions to S and bound them in the small time window. The final step is showing that if we make assumptions on the distributions of q and b, we can extend the small time window to infinity, thus giving bounded global solutions to (2.1) - (2.3). In addition to being an interesting mathematical question, global existence is a significant result for the asymptotic scaling

section since it tells us that approximations that favour long time scales are valid.

In Chapter 3, we went through four different approximations to the system derived (2.1) - (2.3) in Chapter 1. The first two approximations explicitly rescaled space-time, based on the argument that most of the parameters are on the level of individual cells, but we are interested in population-level dynamics that play out over timescales that are orders of magnitude larger than the cell level dynamics. First visiting the parabolic scaling, where diffusion effects dominate, we obtained an advection-diffusion type equation (3.16), similar to the classical Keller Segel equation (2.4). Next, is the hyperbolic scaling, where we have a pure advection equation (3.64) caused by a clear directional cue, induced by q, but the equation had no dependence on the chemoattractant. To view the effect of the chemoattractant, we developed higher-order corrections to the equation (3.63). We also pursued another angle, the case of large chemoattractant sensing, and gained another pure advection equation dependent on $\mathbb{E}_T$ (3.64). For both of the scalings, we were able to show that in the limit of the small parameter ϵ, the kinetic equation indeed approaches the limiting equation (see *Theorem* 3 for the parabolic scaling, and *Theorem* 4 for hyperbolic scaling).

After the rescalings come the moment closures, where the kinetic equation is rewritten as an infinite set of equations for statistical quantities (moments). To close the system, we approximate the second moment by some combination of the lower moments, thus closing the moments. The first moment closure we examined was the L^2 moment closure, where the second moment is approximated by minimizing the L^2 norm. This moment closure has the effect of minimizing the oscillations at every level and is the only limiting equation with no anisotropic terms (3.89)-(3.90). The limiting equation has some historical importance, as it is the same as the Cattaneo model. Taking the L^2 moment system further by having the first moment relax quickly to its equilibrium, gives us an advection-diffusion equation similar to the parabolic scaling case, except for the notable absence of the anisotropic diffusion (3.95). Finally, there is the equilibrium closure, where the second moment is calculated at the equilibrium. The result of this process is a system of equations much like

the L^2 closure case, except the anisotropic diffusion is recovered, and there is a multitude of additional terms that represent the interaction between the chemoattractant and the fibre distribution, as well as chemoattractant with itself (3.108). We also assume that the first moment relaxes quickly to the equilibrium, and we once again gain an advection-diffusion equation (3.112), that in the case of the interaction terms being small coincides with the parabolic limit equation.

Chapter 4 aims to visualize these solutions for endothelial cells, forming a vascular network. Since we were interested in the system's long time behaviour to see the network like structures, we examined the parabolic scaling. To numerically solve (3.33), we had to be careful of the advection term, as well as the anisotropic terms. For this reason, we went with a semidiscrete hybrid finite element/difference method. Using this numerical scheme, we went through numerous experiments; the first experiment we did was to recreate the vascular network assembly results in [47, 20], using the parabolic scaling. We were able to match our solutions to theirs qualitatively; our ability to do this suggests that the flux rapidly relaxes to the equilibrium in their hyperbolic models. For the other experiments, we explored the effects of anisotropic diffusion and the chemotactic velocity mixing. For the anisotropic diffusion, the effect is essentially smearing the cells along the fibre direction, since movement along those directions is favoured. The chemotactic velocity had the opposite effect. The mixing dissuaded movement along directions, but unaffected diffusion along its complement, retrieving similar results as the anisotropic diffusion. The last experiment we looked at was both the anisotropic diffusion and the chemotactic mixing, which lead to a mixed regime set up. In regions with low cell density, the anisotropic diffusion would dominate, but the chemotactic velocity would govern the motion in high-density regions.

The kinetic chemotaxis system has various mathematical challenges, particularly concerning global existence. We had to make major simplifications to our system by reducing the fibre distributions' dependence from a functional dependence on the density to just a dependence on the velocity. It would be impressive to extend our global existence result to a class of functions on ρ. The difficulty arises from how we arrive at our bound for P, which requires the

kinetic equation to have a certain symmetry, that is translation by q. Another mathematical difficulty was deriving error estimates for the moment closure methods. In [26], Hillen was able to show that the error between the kinetic chemotaxis system and the Cattaneo system was proportional to $\|\nabla\rho_0\|_2$. We were unable to obtain such a result for closure systems due to the non-linearity in the $\mathbb{E}_T$ term for the L^2 model, and the interaction terms for the Equilibrium closure model.

Now, where does this article fit into the existing chemotaxis literature? In this paper, we looked at the kinetic chemotaxis model on the torus with volume filling term, which puts us at odds with most of the kinetic chemotaxis literature. Most work on the kinetic chemotaxis literature focuses on the problem in $\mathbb{R}^n$ on altering the chemotactic gradient to a nonlocal version or using a cell density control on the gradient [32, 5, 11]. The closest result to ours is the paper by Hillen and Painter [27], where they show the global existence of Keller-Segel type equation with volume filling term on compact manifolds. Since they were looking exclusively at the chemotaxis equation's parabolic scaling, the mathematical differences are quite substantial. These differences are visible in the availability of *a priori* bounds of the cell density for bounded chemotactic gradient, whereas the P can only be bounded through positivity or mass conservation [43]. This paper also gives a novel summary of the common approximation methods for the kinetic equations in the chemotaxis context, and we present new proofs for their convergence. We go through the biological implications of the four methods and where they overlap. These overlaps occur in four regimes, the diffusion dominated regime where there is either a little to no directional cue provided by q, a drift-diffusion regime where both the advection and diffusion terms are close to the same magnitude, drift dominated regime where the advection terms control the dynamics, and finally the isotropic case where the anisotropy is minimal. The summary of these approximations provides a useful guide for further biological models involving chemotaxis in more complex environments or sensing scenarios.

Bibliography

[1] Wolgang Alt. Biased random walk Models for chemotaxis and related diffusion approximations. *Journal of Mathematical Biology*, 9(2):147–177, 1980.

[2] Melinda D Baker, Peter M Wolanin, and Jeffry B Stock. Signal transduction in bacterial chemotaxis. *Bioessays*, 28(1):9–22, 2006.

[3] Howard C Berg and Robert A Anderson. Bacteria swim by rotating their flagellar filaments. *Nature*, 245(5425):380–382, 1973.

[4] Howard C Berg and Douglas A Brown. Chemotaxis in escherichia coli analysed by three-dimensional tracking. *Nature*, 239(5374):500–504, 1972.

[5] Nikolaos Bournaveas, Vincent Calvez, Susana Gutiérrez, and Benoît Perthame. Global existence for a kinetic model of chemotaxis via dispersion and Strichartz estimates. *Communications in Partial Differential Equations*, 33(1):79–95, 2008.

[6] Elena O Budrene and Howard C Berg. Complex patterns formed by motile cells of escherichia coli. *Nature*, 349(6310):630–633, 1991.

[7] Elena O Budrene and Howard C Berg. Dynamics of formation of symmetrical patterns by chemotactic bacteria. *Nature*, 376(6535):49–53, 1995.

[8] Carlo Cattaneo. Sulla conduzione del calore. *Atti Sem. Mat. Fis. Univ. Modena*, 3:83–101, 1948.

[9] Carlo Cercignani. The Boltzmann equation. In *The Boltzmann equation and its applications*, pages 40–103. Springer, 1988.

[10] Carlo Cercignani, Reinhard Illner, and Mario Pulvirenti. *The mathematical theory of dilute gases*, volume 106. Springer Science & Business Media, 2013.

[11] Fabio ACC Chalub, Peter A Markowich, Benoît Perthame, and Christian Schmeiser. Kinetic models for chemotaxis and their drift-diffusion limits. In *Nonlinear Differential Equation Models*, pages 123–141. Springer, 2004.

[12] Arnaud Chauviere, Thomas Hillen, and Luigi Preziosi. Modeling cell movement in anisotropic and heterogeneous network tissues. *Networks & Heterogeneous Media*, 2(2):333, 2007.

[13] Alina Chertock, Yekaterina Epshteyn, Hengrui Hu, and Alexander Kurganov. High-order positivity-preserving hybrid finite-volume-finite-difference methods for chemotaxis systems. *Advances in Computational Mathematics*, 44(1):327–350, 2018.

[14] John B Conway. *A course in functional analysis*, volume 96. Springer, 2019.

[15] Lucilla Corrias, Benoît Perthame, and Hatem Zaag. Global solutions of some chemotaxis and angiogenesis systems in high space dimensions. *Milan Journal of Mathematics*, 72(1):1–28, 2004.

[16] Y Dolak and T Hillen. Cattaneo models for chemosensitive movement. numerical solution and pattern formation. *Journal of Mathematical Biology*, 46(2):153–170, 2003.

[17] John R Dormand and Peter J Prince. A family of embedded Runge-Kutta formulae. *Journal of Computational and Applied Mathematics*, 6(1):19–26, 1980.

[18] GA Dunn and JP Heath. A new hypothesis of contact guidance in tissue cells. *Experimental Cell Research*, 101(1):1–14, 1976.

[19] Lawrence C Evans. *Partial differential equations*, volume 19. American Mathematical Soc., 2010.

[20] Francis Filbet, Philippe Laurençot, and Benoît Perthame. Derivation of hyperbolic models for chemosensitive movement. *Journal of Mathematical Biology*, 50(2):189–207, 2005.

[21] R Firtel. Dictyostelium cinema, 2001.

[22] Stefano Guido and Robert T Tranquillo. A methodology for the systematic and quantitative study of cell contact guidance in oriented collagen gels. correlation of fibroblast orientation and gel birefringence. *Journal of Cell Science*, 105(2):317–331, 1993.

[23] Richard Haberman. *Elementary applied partial differential equations*, volume 987. Prentice Hall Englewood Cliffs, NJ, 1983.

[24] KP Hadeler. Reaction telegraph equations and random walk systems. *Stochastic and Spatial Structures of Dynamical Systems*, 45:133, 1996.

[25] T Hillen. On the L^2-moment closure of transport equations: The general case. *Discrete & Continuous Dynamical Systems-B*, 5(2):299, 2005.

[26] Thomas Hillen. On the L^2-moment closure of transport equations: The Cattaneo approximation. *Discrete & Continuous Dynamical Systems-B*, 4(4):961, 2004.

[27] Thomas Hillen and Kevin Painter. Global existence for a parabolic chemotaxis model with prevention of overcrowding. *Advances in Applied Mathematics*, 26(4):280–301, 2001.

[28] Thomas Hillen, Kevin Painter, and Christian Schmeiser. Global existence for chemotaxis with finite sampling radius. *Discrete & Continuous Dynamical Systems-B*, 7(1):125, 2007.

[29] Thomas Hillen and Kevin J Painter. Transport and anisotropic diffusion models for movement in oriented habitats. In *Dispersal, individual movement and spatial ecology*, pages 177–222. Springer, 2013.

[30] Thomas Hillen, Kevin J Painter, Amanda C Swan, and Albert D Murtha. Moments of von Mises and Fisher distributions and applications. *Mathematical Biosciences & Engineering*, 14(3):673–694, 2017.

[31] Greg Huber. Gamma function derivation of n-sphere volumes. *The American Mathematical Monthly*, 89(5):301–302, 1982.

[32] Hyung Ju Hwang, Kyungkeun Kang, and Angela Stevens. Global solutions of nonlinear transport equations for chemosensitive movement. *SIAM Journal on Mathematical Analysis*, 36(4):1177–1199, 2005.

[33] Willi Jäger and Stephan Luckhaus. On explosions of solutions to a system of partial differential equations modelling chemotaxis. *Transactions of the American Mathematical Society*, 329(2):819–824, 1992.

[34] Daniel D Joseph and Luigi Preziosi. Heat waves. *Reviews of Modern Physics*, 61(1):41, 1989.

[35] Evelyn F Keller and Lee A Segel. Initiation of slime mold aggregation viewed as an instability. *Journal of Theoretical Biology*, 26(3):399–415, 1970.

[36] Knut-Andreas Lie and Sebastian Noelle. On the artificial compression method for second-order nonoscillatory central difference schemes for systems of conservation laws. *SIAM Journal on Scientific Computing*, 24(4):1157–1174, 2003.

[37] Yves A Muller, Hans W Christinger, Bruce A Keyt, and Abraham M de Vos. The crystal structure of vascular endothelial growth factor (vegf) refined to 1.93 å resolution: multiple copy flexibility and receptor binding. *Structure*, 5(10):1325–1338, 1997.

[38] Frank WJ Olver, Daniel W Lozier, Ronald F Boisvert, and Charles W Clark. *NIST handbook of mathematical functions hardback and CD-ROM*. Cambridge University Press, 2010.

[39] Hans G Othmer, Steven R Dunbar, and Wolfgang Alt. Models of dispersal in biological systems. *Journal of Mathematical Biology*, 26(3):263–298, 1988.

[40] Hans G Othmer and Thomas Hillen. The diffusion limit of transport equations derived from velocity-jump processes. *SIAM Journal on Applied Mathematics*, 61(3):751–775, 2000.

[41] Floriano Papi, Paolo Luschi, S Akesson, S Capogrossi, and GC Hays. Open-sea migration of magnetically disturbed sea turtles. *Journal of Experimental Biology*, 203(22):3435–3443, 2000.

[42] Amnon Pazy. *Semigroups of linear operators and applications to partial differential equations*, volume 44. Springer Science & Business Media, 2012.

[43] Benoît Perthame. *Kinetic formulation of conservation laws*, volume 21. Oxford University Press, 2002.

[44] Benoît Perthame. *Transport equations in biology*. Springer Science & Business Media, 2006.

[45] Alain Pluen, Paolo A Netti, Rakesh K Jain, and David A Berk. Diffusion of macromolecules in agarose gels: comparison of linear and globular configurations. *Biophysical Journal*, 77(1):542–552, 1999.

[46] Mercedes A Rivero, Robert T Tranquillo, Helen M Buettner, and Douglas A Lauffenburger. Transport models for chemotactic cell populations based on individual cell behavior. *Chemical Engineering Science*, 44(12):2881–2897, 1989.

[47] Guido Serini, Davide Ambrosi, Enrico Giraudo, Andrea Gamba, Luigi Preziosi, and Federico Bussolino. Modeling the early stages of vascular network assembly. *The EMBO Journal*, 22(8):1771–1779, 2003.

[48] CYNTHIA L Stokes, DOUGLAS A Lauffenburger, and STUART K Williams. Migration of individual microvessel endothelial cells: stochastic model and parameter measurement. *Journal of Cell Science*, 99(2):419–430, 1991.

[49] Daniel W Stroock. Some stochastic processes which arise from a model of the motion of a bacterium. *Zeitschrift für Wahrscheinlichkeitstheorie und verwandte Gebiete*, 28(4):305–315, 1974.

[50] Peter K Sweby. High resolution schemes using flux limiters for hyperbolic conservation laws. *SIAM Journal on Numerical Analysis*, 21(5):995–1011, 1984.

[51] Terence Tao. *Higher order Fourier analysis*, volume 142. American Mathematical Soc., 2012.

[52] Ryan J Thiessen and Alexei F Cheviakov. Nonlinear dynamics of a viscous bubbly fluid. *Communications in Nonlinear Science and Numerical Simulation*, 73:244–264, 2019.

[53] Bram Van Leer. Towards the ultimate conservative difference scheme. v. a second-order sequel to Godunov's method. *Journal of Computational Physics*, 32(1):101–136, 1979.

[54] Mark R Walter, William J Cook, Steven E Ealick, Tattanahalli L Nagabhushan, Paul P Trotta, and Charles E Bugg. Three-dimensional structure of recombinant human granulocyte-macrophage colony-stimulating factor. *Journal of Molecular Biology*, 224(4):1075–1085, 1992.

[55] Xuefeng Wang. Qualitative behavior of solutions of chemotactic diffusion systems: effects of motility and chemotaxis and dynamics. *SIAM Journal on Mathematical Analysis*, 31(3):535–560, 2000.

[56] Eric W Weisstein. Fourier transform-gaussian. *Wolfram Web Resource. http://mathworld. wolfram. com*, 2013.

[57] DE Woodward, R Tyson, MR Myerscough, JD Murray, EO Budrene, and HC Berg. Spatio-temporal patterns generated by salmonella typhimurium. *Biophysical Journal*, 68(5):2181–2189, 1995.